

# GOLDMAN-TURAEV FORMALITY FROM THE KONTSEVITCH INTEGRAL

DROR BAR-NATAN, ZSUZSANNA DANCOS, TAMARA HOGAN, JESSICA LIU,  
AND NANCY SCHERICH

ABSTRACT. We present a three dimensional realisation of the Goldman-Turaev Lie bialgebra, and construct Goldman-Turaev homomorphic expansions from the Kontsevich integral.

## CONTENTS

1. Introduction	2
1.1. Motivation	3
2. Conceptual summary	4
3. Preliminaries: Homomorphic expansions and the Goldman-Turaev Lie bialgebra	7
3.1. Homomorphic expansions and the framed Kontsevich integral	7
3.2. The Goldman-Turaev Lie bialgebra	10
3.3. Associated graded Goldman-Turaev Lie bialgebra	13
4. Expansions for tangles in handlebodies	16
4.1. Framed oriented tangles	16
4.2. Operations on $\tilde{\mathcal{T}}$	19
4.3. The $t$ -filtration on $\tilde{\mathcal{T}}$ and the associated graded $\tilde{\mathcal{A}}$	19
4.4. Operations on $\tilde{\mathcal{A}}$	22
4.5. The $s$ -filtration on $\tilde{\mathcal{T}}$ and $\tilde{\mathcal{A}}$	23
4.6. The Conway quotient	24
4.7. Notation conventions	28
5. Identifying the Goldman-Turaev Lie bialgebra	29
5.1. The Goldman Bracket	29
5.2. The Turaev co-bracket	38
References	49

---

*Key words and phrases.* knots, links in a handlebody, expansions, finite type invariants, Lie algebras .

To do list for Zsuzsi

- (1) Section 3.3, there is an old note from Jessica about signs. Do we need to keep that comment, or can we delete it?

## 1. INTRODUCTION

In 1986, Goldman defined a Lie bracket [Gol86] on the space of homotopy classes of free loops on a compact oriented surface. Shortly after in 1991, Turaev defined a cobracket [Tur91] on the same space<sup>1</sup>. This bracket and cobracket make the space of free loops into a Lie bialgebra – known as the Goldman–Turaev Lie bialgebra – which forms the basis for the field of string topology [?] and has been an object of study from many perspectives.

In this paper we, describe a 3-dimensional lift of the Goldman–Turaev Lie bialgebra into a space of tangles in a handlebody. We recover the bracket and cobracket maps as projections of intuitive operations on tangles. We show the Kontsevich integral is homomorphic with respect to these tangle operations. Our main result is informally summarised as follows:

**Main Result.** *Let  $\tilde{\mathcal{T}}$  denote the space of formal linear combinations of tangles in a punctured disc cross an interval  $M_p = D_p \times I$ . Projecting to the bottom  $D_p \times 0$ , one obtains curves on a punctured disc, and the Goldman–Turaev operations on these curves are induced<sup>2</sup> by the stacking and flipping operations on the tangles. The Kontsevich integral is a homomorphic expansion for tangles in  $M_p$ , and descends to a Goldman–Turaev homomorphic expansion on  $D_p$ .*

This result is parallel to Massuyeau’s [Mas18], however, our approach to the co-bracket is significantly different and simpler, hence, more likely to give insight into the motivational application described below. Another related result is [?], which constructs Goldman–Turaev expansions from the Khnizhnik–Zamolodchikov connection, a geometric incarnation of the Kontsevich integral.

In more detail, we describe a space  $\tilde{\mathcal{T}}$  of formal linear combinations of framed tangles in the handlebody  $\mathcal{D}_p \times I$  and operations on this space, which induce the Goldman–Turaev operations in the bottom projection to  $D_p \times \{0\}$ . The Goldman bracket arises from the commutator associated to the stacking product in a Conway skein quotient of  $\tilde{\mathcal{T}}$ , defined in Section 4.6, and the Turaev cobracketed from taking the difference between a tangle and its vertical flip, again in a Conway quotient. We study the associated graded spaces and operations, and show that the Kontsevich integral is a homomorphic expansion for these tangles, in other words, intertwines the operations with their associated graded counterparts. We show that therefore, the Kontsevich integral descends to a homomorphic expansion for the Goldman–Turaev Lie bialgebra. For the flipping operation and the

<sup>1</sup>Turaev’s version required factoring out by the constant loop; there is a lift to the full space of homotopy classes of loops, given a framing on the surface [AKKN20].

<sup>2</sup>In a specific sense defined in Section 2

Turaev cobracket, the precise statements are subtle, and care needs to be taken with the technical details.

**1.1. Motivation.** The Kashiwara–Vergne equations originally arose from the study of convolutions on Lie groups [?]. The equations were reformulated algebraically in terms of automorphisms of free Lie algebras [?], in this form they are a refinement of the Baker–Campbell–Hausdorff formula for products of exponentials of non-commuting variables.

Kashiwara–Vergne theory has multiple topological interpretations in which Kashiwara–Vergne solutions correspond to certain invariants – called *homomorphic expansions* – of topological objects. The existence of a homomorphic expansion is also called *formality* in the literature, this language is inspired by rational homotopy theory and group theory [?].

One of these topological interpretations is due to the first two authors [BND17], who showed that homomorphic expansions of welded foams – a class of 4-dimensional tangles – are in one to one correspondence with solutions to the KV equations. Recently, a series of papers by Alekseev, Kawazumi, Kuno and Naef [AKKN20, AKKN18b, AKKN18a] drew an analogous connection between KV solutions and homomorphic expansions for the Goldman–Turaev Lie bialgebra for the disc with two punctures (up to non-negligible differences in the technical details). This correspondence was used to generalise the Kashiwara–Vergne equations via considering different surfaces, including those of higher genus.

In other words, there is an intricate algebraic connection between four-dimensional welded foams and the Goldman–Turaev Lie bi-algebra, which strongly suggests that there is a topological connection as well. In addition to the inherent interest in tangles in handlebodies, one goal for this paper is to work towards this connection between the two-dimensional Goldman–Turaev Lie bialgebra and four-dimensional welded foams, by constructing a three-dimensional realisation of the Goldman–Turaev Lie bialgebra, with homomorphic expansions which descend to Goldman–Turaev expansions.

*The paper is organised as follows:* Section 2 gives a general algebraic framework for how the Goldman–Turaev operations are induced by tangle operations. In Section 3 we give a brief overview of the Kontsevich integral and the Goldman–Turaev Lie bialgebra. In Section 4, we define tangles in handlebodies, relevant operations and Vassiliev filtrations. We identify the associated graded space of tangles as a space of chord diagrams, and introduce the Conway skein quotient. In Section 5, we identify the Goldman–Turaev Lie bi-algebra in a low filtration degree, and prove the main theorem.

*Acknowledgements.* We are grateful to Anton Alekseev, Gwenel Massuyeau, and Yusuke Kuno for fruitful conversations. DBN was supported by NSERC RGPIN 262178 and RGPIN-2018-04350, and by The Chu Family Foundation (NYC). ZD was partially supported by the ARC DECRA DE170101128. NS was supported by the NSF under Grant No. DMS-1929284 while in residence at the Institute for

There are other papers by Turaev and Massuyeau–Turaev that are not mentioned here. There are also some references that Yusuke mentioned that we should include

Computational and Experimental Research in Mathematics in Providence, RI, during the Braids Program. We thank the Sydney Mathematical Research Institute and the University of Sydney for their hospitality, and funding for multiple research visits.

## 2. CONCEPTUAL SUMMARY

sec:conceptsum

We induce the genus zero Goldman-Turaev operations from tangle operations, in the spirit of “connecting homomorphisms”: this Section is a summary of the basic approach. We provide some proofs which are not immediate and use the words *homomorphic expansions*, and *Goldman-Turaev operations* without definition, only mentioning their basic properties which make this conceptual outline coherent; the definitions follow in Section 3.

In the diagram (2.1), the top and bottom rows are exact and the right and left vertical maps are zero, and therefore, by minor diagram chasing, the middle vertical map  $\lambda$  induces a unique map  $\eta : C \rightarrow D$ , a degenerate case of a connecting homomorphism. In our applications  $\lambda$  is a difference of two maps  $\lambda_1$  and  $\lambda_2$ , whose values differ in  $E$  but coincide in a quotient  $F$ .

eq:inducedconnhom

$$\begin{array}{ccccccc}
 & & & \eta & & & \\
 & & & \text{---} & & & \\
 A & \longrightarrow & B & \longrightarrow & C & \longrightarrow & 0 \\
 \downarrow 0 & & \downarrow \lambda = \lambda_1 - \lambda_2 & & \downarrow 0 & & \\
 0 & \longrightarrow & D & \longrightarrow & E & \longrightarrow & F
 \end{array}
 \tag{2.1}$$

In Section 5 we present two constructions which produce the Goldman bracket and the Turaev cobracket, respectively, as induced homomorphisms  $\eta$ , from corresponding tangle operations  $\lambda_1$  and  $\lambda_2$ . The following example is a schematic version of what will become the argument for the Goldman bracket.

**Example 2.1.** Let  $A$  be an associative algebra, and let  $\{L_i\}$  denote the lower central series of  $A$ . That is,  $L_1 := A$ , and  $L_{i+1} := [L_i, A]$ . Then the  $L_i$  are Lie ideals, and let  $M_i = AL_i = L_iA$  denote the two-sided ideal generated by  $L_i$ . The quotient  $A/M_1$  is the abelianisation of  $A$ , denoted by  $A^{ab}$ . Then we have the following diagram:

eq:SnakeExample

$$\begin{array}{ccccccc}
 0 & \longrightarrow & K & \longrightarrow & \frac{A}{M_2} \otimes \frac{A}{M_2} & \longrightarrow & A^{ab} \otimes A^{ab} \longrightarrow 0 \\
 \downarrow 0 & & \downarrow [\cdot, \cdot] & & \downarrow 0 & & \\
 0 & \longrightarrow & \frac{M_1}{M_2} & \longrightarrow & \frac{A}{M_2} & \longrightarrow & A^{ab} \longrightarrow 0
 \end{array}
 \tag{2.2}$$

Here  $\lambda$  is the algebra commutator, which is indeed the difference between two maps: the multiplication  $(\lambda_1)$  and the multiplication in the opposite order  $(\lambda_2)$ . The kernel  $K$  of the projection to  $A^{ab} \otimes A^{ab}$  is generated by the subalgebras  $\left\{ \frac{M_1}{M_2} \otimes \frac{A}{M_2}, \frac{A}{M_2} \otimes \frac{M_1}{M_2} \right\}$  in  $\frac{A}{M_2} \otimes \frac{A}{M_2}$ . The map  $\eta$  is a well defined commutator map  $A^{ab} \otimes A^{ab} \rightarrow \frac{M_1}{M_2}$ , given by  $\eta(x \otimes y) = [x, y] \bmod M_2$ .  $\square$

The goal of this paper is to construct homomorphic expansions (aka formality isomorphisms) for the Goldman-Turaev Lie bialgebra from the Kontsevich integral. In outline, this follows from the naturality property of the construction above, under the associated graded functor, as follows.

Given a short exact sequence

$$0 \longrightarrow A \xhookrightarrow{\iota} B \twoheadrightarrow^{\pi} C \longrightarrow 0,$$

and a descending filtration on  $B$

$$B = B^0 \supseteq B^1 \supseteq B^2 \supseteq \cdots \supseteq B^n \supseteq \cdots,$$

there is an induced filtration on  $A$  given by

$$A = A^0 \supseteq A^1 \supseteq A^2 \supseteq \cdots \supseteq A^n \supseteq \cdots,$$

where  $A^i = \iota^{-1}(\iota A \cap B^i)$ . Similarly, there is an induced filtration on  $C$  given by

$$C = C^0 \supseteq C^1 \supseteq C^2 \supseteq \cdots \supseteq C^n \supseteq \cdots$$

where  $C^i = \pi(B^i)$ .

**Lemma 2.2.** *If the rows of the diagram (2.1) are exact and filtered so that the filtrations on the left and right are induced from the filtration in the middle, then the induced map  $\eta$  is also filtered.*

*Proof.* Basic diagram chasing: given  $c \in C^n$ , since  $C^n = \pi(B^n)$ , there is a  $b \in B^n$  such that  $\pi(b) = c$ . Since  $\lambda$  is filtered,  $\lambda(b) \in E^n$ , and  $\lambda(b) \in \iota(D)$  by exactness. Since  $D^n = \iota^{-1}(\iota(D) \cap E^n)$ , we have that  $\lambda(b) = \iota(d)$  for a  $d \in D^n$ . By uniqueness of the induced map,  $d = \eta(c)$ .  $\square$

The associated graded functor is a functor from the category of filtered algebras (or vector spaces) to the category of graded algebras (or vector spaces). For a filtered algebra

$$A = A^0 \supseteq A^1 \supseteq A^2 \supseteq \cdots \supseteq A^n \supseteq \cdots,$$

the (degree completed) associated graded algebra is defined to be

$$\text{gr } A = \prod_{n=0}^{\infty} A^n / A^{n+1}.$$

The associated graded map of a filtered map is defined in the natural way (as in the proof of Lemma 2.3 below). In general,  $\text{gr}$  is not an exact functor, but it does preserve exactness for the special class of filtered short exact sequences where the filtrations on  $A$  and  $C$  are induced from the filtration on  $B$ :

lem:ExagtGr

**Lemma 2.3.** *If in the filtered short exact sequence*

$$0 \longrightarrow A \xrightarrow{\iota} B \xrightarrow{\pi} C \longrightarrow 0$$

*the filtrations on  $A$  and  $C$  are induced from the filtration on  $B$ , then the associated graded sequence is also exact:*

$$0 \longrightarrow \text{gr } A \xrightarrow{\text{gr } \iota} \text{gr } B \xrightarrow{\text{gr } \pi} \text{gr } C \longrightarrow 0.$$

*Proof.* Since  $\text{gr}$  is a functor, we know that  $\text{gr } \pi \circ \text{gr } \iota = 0$ , hence  $\text{im } \text{gr } \iota \subseteq \ker \text{gr } \pi$ . It remains to show that  $\ker \text{gr } \pi \subseteq \text{im } \text{gr } \iota$ .

Let  $[b] \in B^n/B^{n+1}$ , and assume that  $\text{gr } \pi([b]) = 0$ . Since  $\text{gr } \pi([b]) = [\pi(b)] \in C^n/C^{n+1}$ , we have  $\text{gr } \pi([b]) = 0$  if and only if  $\pi(b) \in C^{n+1}$ . As the filtration on  $C$  is induced from  $B$ , we know that  $C^{n+1} = \pi(B^{n+1})$ . Thus,  $\pi(b) \in \pi(B^{n+1})$ . Or in other words, there exists  $x \in B^{n+1}$  such that  $\pi(b) = \pi(x)$ . This implies that  $\pi(b - x) = 0$  and hence that  $b - x \in \iota(A)$  by exactness.

Therefore,  $b = x + \iota(a)$  for some  $x \in B^{n+1}$  and  $a \in A$ . It follows that  $[b] = [\iota(a)] = \text{gr } \iota([a])$  in  $B^n/B^{n+1}$  and hence  $\ker \text{gr } \pi \subseteq \text{im } \text{gr } \iota$  as required.  $\square$

gr\_induced\_is\_unique

**Corollary 2.4.** *If the rows of the diagram in Equation 2.1 are exact, and the filtrations on the left and right are induced from the filtration in the middle, then the rows of the associated graded diagram are also exact, and the unique connecting homomorphism is  $\text{gr } \eta$ .*

$$(2.3) \quad \begin{array}{ccccccc} 0 & \longrightarrow & \text{gr } A & \longrightarrow & \text{gr } B & \longrightarrow & \text{gr } C \longrightarrow 0 \\ & & \downarrow 0 & & \downarrow \text{gr } \lambda & & \downarrow 0 \\ 0 & \longrightarrow & \text{gr } D & \longrightarrow & \text{gr } E & \longrightarrow & \text{gr } F \longrightarrow 0 \end{array}$$

A dashed curved arrow labeled  $\text{gr } \eta$  points from  $\text{gr } A$  to  $\text{gr } C$ .

*Proof.* The exactness of the rows is Lemma 2.3. The induced map is  $\text{gr } \eta$  as  $\text{gr } \eta$  makes the diagram commute, and the induced map is unique.  $\square$

An expansion for an algebraic structure  $X$  is a filtered homomorphism  $Z : X \rightarrow \text{gr } X$  (with special properties as explained in Section 3.1). Thus, if expansions exist for each of the spaces  $A$  through  $F$ , we obtain a multi-cube:

eq:Cube

$$\begin{array}{ccccccc}
 & & A & \xrightarrow{\quad} & B & \xrightarrow{\quad} & C \rightarrow 0 \\
 & \swarrow & \downarrow Z_A & \swarrow \lambda & \downarrow Z_B & \swarrow & \downarrow Z_C \\
 0 \rightarrow & D & \xrightarrow{\quad} & E & \xrightarrow{\quad} & F & \\
 & \downarrow Z_D & \swarrow & \downarrow Z_E & \swarrow & \downarrow Z_F & \\
 & \text{gr } D & \xrightarrow{\quad} & \text{gr } E & \xrightarrow{\quad} & \text{gr } F & \rightarrow 0 \\
 & & \swarrow & \swarrow \text{gr } \lambda & \swarrow & & \\
 & & & & & & 
 \end{array}$$

$\eta$  (top dashed arrow from  $D$  to  $C$ )  
 $\text{gr } \eta$  (bottom dashed arrow from  $\text{gr } D$  to  $\text{gr } F$ )

(2.4)

lem:Naturality

**Lemma 2.5.** *If, in the multi-cube (2.4) all vertical faces commute, then so does the square:*

eq:HomExp

(2.5)

$$\begin{array}{ccc}
 D & \xleftarrow{\quad \eta \quad} & C \\
 \downarrow Z_D & & \downarrow Z_C \\
 \text{gr } D & \xleftarrow{\quad \text{gr } \eta \quad} & \text{gr } C
 \end{array}$$

*Proof.* Follows from the uniqueness of the induced maps.  $\square$

In Section 5.1, we will show how the Goldman bracket and Turaev cobracket each arise as induced maps  $\eta$ , where  $\lambda = \lambda_1 - \lambda_2$  is a difference of tangle operations. Therefore the Kontsevich integral therefore induces an expansion for the Goldman–Turaev operations, and the commutativity of the square (2.5) for each operation is – by definition – the homomorphicity property of the expansion. This homomorphicity is our main result. The non-trivial vertical face of the multi-cube is the one containing  $\lambda$ , and the commutativity of this for each Goldman–Turaev operation will follow from homomorphicity properties of the Kontsevich integral. Namely, the Kontsevich integral (standing in for  $Z_B$  and  $Z_E$ ) intertwines the appropriate tangle operations  $\lambda_0$  and  $\lambda_1$  with their associated graded counterparts. This is the idea behind the approach of this paper.

### 3. PRELIMINARIES: HOMOMORPHIC EXPANSIONS AND THE GOLDMAN-TURAEV LIE BIALGEBRA

subeseFrmedKma

**3.1. Homomorphic expansions and the framed Kontsevich integral.** The Kontsevich Integral is the knot theoretic prototype of a *homomorphic expansion*. Homomorphic expansions (a.k.a. formality isomorphisms, well-behaved universal finite type invariants) provide a connection between knot theory and quantum algebra/Lie theory. We begin with a short review of homomorphic expansions

from an algebraic perspective, which is outlined – in a slightly different, finitely presentated case – in [BND17, Section 2]. Kontsevich’s original construction gives an invariant of unframed links; for a detailed introduction, we recommend [CDM12, Section 8], or [Kon93, BN95, Dan10]. In this paper we work primarily with framed links and tangles, thus we briefly review the framed versions of the Vassiliev filtration and Kontsevich integral; for more detail see [CDM12, Sections 3.5 and 9.1] and [LM96].

**3.1.1. Homomorphic expansions.** Let  $\mathcal{K}$  denote a given set of knots, links or tangles in  $\mathbb{R}^3$  (e.g., oriented knots), and allow formal linear combinations with coefficients in  $\mathbb{C}$ . For links and tangles, allow only linear combinations of embeddings of the same skeleton<sup>3</sup>. The *Vassiliev filtration* (defined in terms of resolutions of double points  $\mathbb{X} = \mathbb{X}^+ - \mathbb{X}^-$ ) is a decreasing filtration on this linear extension:

$$\mathbb{C}\mathcal{K} = \mathcal{K}_0 \supseteq \mathcal{K}_1 \supseteq \mathcal{K}_2 \supseteq \dots$$

The degree completed associated graded space of  $\mathbb{C}\mathcal{K}$  with respect to the Vassiliev filtration is

$$\mathcal{A} := \prod_{n \geq 0} \mathcal{K}_n / \mathcal{K}_{n+1}.$$

An *expansion* is a filtered linear map  $Z : \mathbb{C}\mathcal{K} \rightarrow \mathcal{A}$ , such that the associated graded map of  $Z$  is the identity  $\text{gr } Z = \text{id}_{\mathcal{A}}$ .

Usually,  $\mathcal{K}$  is equipped with additional operations: examples are knot connected sum, tangle composition, strand orientation reversal, etc. Homomorphic expansions are compatible with these operations, and thus allow for a study of  $\mathcal{K}$  via the more tractable associated graded spaces.

Specifically, an expansion is *homomorphic* with respect to an operation  $m$ , if it intertwines  $m$  with its associated graded operation on  $\mathcal{A}$ . That is,  $Z \circ m = \text{gr } m \circ Z$ . A crucial step towards making effective use of this machinery is to get a handle on the space  $\mathcal{A}$  in concrete terms: for example, in classical knot theory,  $\mathcal{A}$  has a combinatorial description as a space of *chord diagrams* [CDM12, Chapter 4].

There is a natural map  $\psi$  from chord diagrams with  $i$  chords to  $\mathcal{K}_i / \mathcal{K}_{i+1}$ , defined by “contracting chords” as in Figure 1. It is not difficult to establish that  $\psi$  is surjective. In the case of classical (oriented, unframed) knots, there are two relations in the kernel of  $\psi$ : the 4-Term (4T) and Framing Independence (FI) relations, shown in Figure 2. In fact, these two relations generate the kernel, and  $\psi$  descends to an isomorphism on the quotient; this, however, is significantly harder to prove.

The key technique is to construct an expansion as in the following Lemma, [BND17, Proposition 2.7]:

<sup>3</sup>The *skeleton* of a knotted object is the underlying combinatorial object. For example: the skeleton of a link is the number of components; the skeleton of a braid is the underlying permutation; the skeleton of a tangle is the number of strands, connectivity, and number of circle components. In these contexts  $\mathbb{C}\mathcal{K}$  is a disjoint union of vector spaces, rather than a single vector space.





FIGURE 1. Example of  $\psi$  mapping a chord diagram to a knot with double points by contracting the chords. The right-hand side represents a well-defined element in  $\mathcal{K}_3/\mathcal{K}_4$ .

fig:psionchord

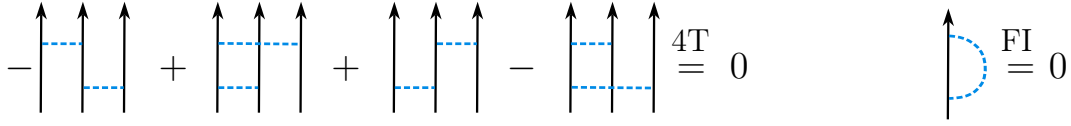


FIGURE 2. The 4T and FI relations, understood as local relations: the strand(s) are part(s) of the skeleton circle, and the skeleton may support additional chords outside the picture shown.

fig:4TFI

lem:assocgradyoga

**Lemma 3.1.** [BND17] Let  $\mathbb{CK}$  be a filtered vector space (or union of vector spaces), and  $\mathcal{A}$  the associated graded space of  $\mathbb{CK}$ . Let  $\mathcal{C}$  be a “candidate model” for  $\mathcal{A}$ : a graded linear space equipped with a surjective homogeneous map  $\psi : \mathcal{C} \rightarrow \mathcal{A}$ . If there exists a filtered map  $Z : \mathbb{CK} \rightarrow \mathcal{C}$ , such that  $\psi \circ \text{gr } Z = \text{id}_{\mathcal{A}}$ , then  $\psi$  is an isomorphism and  $\psi \circ Z$  is an expansion for  $\mathcal{K}$ .

$$\begin{array}{ccc}
 \mathbb{CK} & \xrightarrow{Z} & \mathcal{C} \\
 & & \downarrow \psi \\
 & & \mathcal{A}
 \end{array}
 \quad \xRightarrow{\text{gr}} \quad
 \begin{array}{ccc}
 \mathcal{A} & \xrightarrow{\text{gr } Z} & \mathcal{C} \\
 \swarrow \psi \circ \text{gr } Z = \text{id}_{\mathcal{A}} & & \downarrow \psi \\
 & & \mathcal{A}
 \end{array}$$

In other words, once one finds a candidate model  $\mathcal{C}$  for  $\mathcal{A}$ , finding an *expansion valued in  $\mathcal{C}$*  also implies that  $\psi$  is an isomorphism. In classical Vassiliev theory,  $\mathcal{K}$  is the space of oriented knots,  $\mathcal{C}$  is the space of chord diagrams, and a  $\mathcal{C}$ -valued expansion is the Kontsevich integral [Kon93].

subsubsec:Framing

**3.1.2. Framed theory.** In this paper we work with *framed* links and tangles, so we give a brief introduction to the framed version of the general theory summarised in the previous section. For simplicity, we consider links for now.

Let  $\mathcal{K}$  denote the set of *framed* links in  $\mathbb{R}^3$ : that is, links along with a non-zero section of the normal bundle. A link diagram is interpreted as a framed link using the blackboard framing. The Reidemeister move R1 move changes the blackboard

framing, and by omitting it, one obtains a Reidemeister theory for framed links. In analogy with a double point, a *framing change* is defined to be the difference

$$\uparrow := \uparrow\!\!\!\circ - \uparrow.$$

The framed Vassiliev filtration is the descending filtration

$$\tilde{\mathcal{K}} = \tilde{\mathcal{K}}_0 \supseteq \tilde{\mathcal{K}}_1 \supseteq \tilde{\mathcal{K}}_2 \supseteq \dots$$

where  $\tilde{\mathcal{K}}_i$  is linearly generated by knots with at least  $i$  double points *or framing changes*. The degree completed associated graded space of  $\tilde{\mathcal{K}}$  with respect to the framed Vassiliev filtration is

$$\tilde{\mathcal{A}} := \prod_{n \geq 0} \tilde{\mathcal{K}}_n / \tilde{\mathcal{K}}_{n+1}.$$

A natural first guess for a combinatorial description of  $\tilde{\mathcal{A}}$  is in terms of chord diagrams with “framing change markings”  $\uparrow\!\!\!\circ$  on the skeleton, graded by the number of chords and markings. There is a natural surjective graded map  $\tilde{\psi}$  from marked chord diagrams onto  $\tilde{\mathcal{A}}$ , which contracts chords as in the classical case, and which replaces each marking  $\uparrow\!\!\!\circ$  with a framing change  $\uparrow$ . The kernel of  $\tilde{\psi}$  includes the  $4T$  relation as before.

In place of the  $FI$  relation ( $\uparrow\!\!\!\circ = 0$ ), a weaker relation arises from the equality  $\uparrow\!\!\!\circ - \uparrow\!\!\!\circ = \uparrow\!\!\!\circ - \uparrow\!\!\!\circ = (\uparrow\!\!\!\circ - \uparrow) + (\uparrow - \uparrow\!\!\!\circ)$ , and  $\uparrow - \uparrow\!\!\!\circ = \uparrow\!\!\!\circ - \uparrow$  modulo  $\tilde{\mathcal{K}}_2$ . In other words, the following relation is in the kernel of  $\tilde{\psi}$ :

$$\uparrow\!\!\!\circ = 2 \uparrow\!\!\!\circ.$$

Therefore, it is not necessary to have dedicated notation for the framing change markings, since  $\uparrow\!\!\!\circ = \frac{1}{2} \uparrow\!\!\!\circ$ . The candidate model for the associated graded space is simply chord diagrams modulo the  $4T$  relation, and no  $FI$  relation. We denote this space by  $\tilde{\mathcal{C}}$ .

To show that  $\tilde{\psi} : \tilde{\mathcal{C}} \rightarrow \tilde{\mathcal{A}}$  is an isomorphism, it is enough to construct a  $\tilde{\mathcal{C}}$ -valued expansion and use Lemma 3.1. This  $\tilde{\mathcal{C}}$ -valued expansion is the framed version  $\tilde{Z}$  of the Kontsevich integral. For details of this construction see [CDM12, Section 9.1], or [LM96, Gor99].

subsec:IntroGT

**3.2. The Goldman-Turaev Lie bialgebra.** In order to define the Goldman-Turaev Lie bialgebra, we need to recall some basic definitions and notation.

Let  $D_p$  denote  $p$ -punctured disc, with  $p+1$  circle boundary components  $\partial_0, \partial_1, \dots, \partial_p$ , embedded in the complex plane so that  $\partial_0$  is the outer boundary, as in Figure 3. In particular, the plane-embedding specifies a framing (trivialisation of the tangent bundle) on  $D_p$ , and thus immersed loops in  $D_p$  are equipped with a notion of *rotation number*.

Let  $\pi = \pi_1(D_p, *)$  denote the fundamental group of  $D_p$  with basepoint  $* \in \partial_0$ . We denote by  $\mathbb{C}\pi$  the group algebra of  $\pi$ .

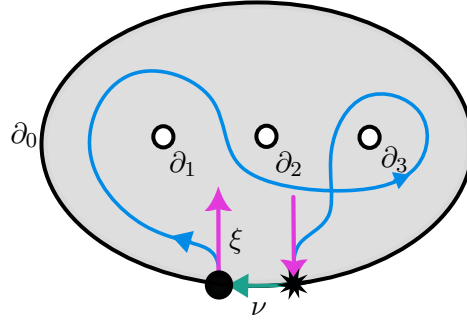


FIGURE 3.  $D_3$  with an immersed loop from  $\bullet$  to  $*$  with initial tangent vector  $\xi$  and terminal tangent vector  $-\xi$ . The path along the boundary from  $*$  to  $\bullet$  is  $\nu$ .

fig:DP

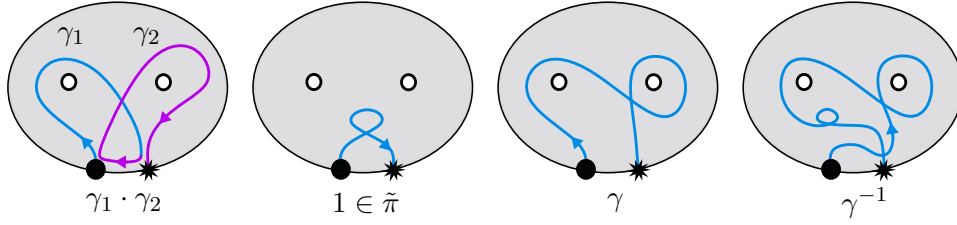


FIGURE 4. The group structure on  $\tilde{\pi}$ .

fig:DPGroup

We also need to consider based paths. Let  $\bullet$  and  $*$  be two “nearby” basepoints on  $\partial_0$  and  $\xi$  be the direction of the inward pointing normal vector to  $\partial_0$  at  $\bullet$  and  $*$ . Let  $\tilde{\pi} = \tilde{\pi}_{\bullet,*}$  denote the set of regular homotopy classes of immersed curves  $\gamma : ([0, 1], 0, 1) \rightarrow (D_p, \bullet, *)$ , so that  $\dot{\gamma}(0) = \xi$ , and  $\dot{\gamma}(1) = -\xi$ , as shown in Figure 3. Note that the rotation number is invariant under regular homotopy. Recall that  $\tilde{\pi}$  is in fact a group, illustrated in Figure 4 and defined as follows:

- (1) Let  $\nu$  denote the path from  $*$  to  $\bullet$  along  $\partial_0$ . The group product  $\gamma_1 \cdot \gamma_2$  is the smooth concatenation of  $\gamma_1$  with  $\nu$  followed by  $\gamma_2$ .
- (2) The group identity is the class of paths which, when composed with  $\nu$ , become contractible loops of rotation number zero.
- (3) The inverse of  $\gamma$  is the concatenation  $\overline{\nu} \overline{\gamma} \nu^*$  where the overline denotes the reverse path, and  $\nu^*$  includes a negative twist (to ensure that the rotation number of  $\gamma \cdot \gamma^{-1}$  is 0). The beginning and end of the path is adjusted in an epsilon neighbourhood of the base points to have inward and outward pointing tangent vectors, as in Figure 4.

Denote by  $\mathbb{C}\tilde{\pi}$  the group algebra of  $\tilde{\pi}$ . There is a forgetful map  $\tilde{\pi} \rightarrow \pi$  which maps  $\gamma$  to the (non-regular) homotopy class of  $\gamma\nu$ . This linearly extends to a forgetful map  $\mathbb{C}\tilde{\pi} \rightarrow \mathbb{C}\pi$ .

For an algebra  $A$  we denote by  $|A|$  the *linear*<sup>4</sup> quotient  $A/[A, A]$ , where  $[A, A]$  denotes the subspace spanned by commutators  $[x, y] = xy - yx$  for  $x, y \in A$ . We denote the quotient (trace) map by  $|\cdot| : A \rightarrow |A|$ . In our context,  $|\mathbb{C}\pi|$  has an explicit description as the  $\mathbb{C}$ -vector space generated by homotopy classes of free loops in  $D_p$ . In a similar but more subtle fashion,  $|\mathbb{C}\tilde{\pi}|$  is spanned by *regular* homotopy classes of immersed free loops, where  $|\gamma|$  denotes the class of  $\gamma\nu$  as a free immersed loop.

The Goldman–Turaev Lie bialgebra comes in two flavours: *original* and *enhanced*. The original construction of the Goldman bracket is a Lie bracket on  $|\mathbb{C}\pi|$ . However, the original Turaev cobracket is only well-defined on  $|\overline{\mathbb{C}\pi}| = |\mathbb{C}\pi|/\mathbb{C}\mathbf{1}$ , the linear quotient by the homotopy class of the constant loop. The space  $|\overline{\mathbb{C}\pi}|$  is a Lie bialgebra with this cobracket and the Goldman bracket, which descends from  $|\mathbb{C}\pi|$ . There is an enhancement [AKKN18b] of the cobracket, which promotes it to  $|\mathbb{C}\pi|$ , thereby making  $|\mathbb{C}\pi|$  a Lie bialgebra under the Goldman bracket and the enhanced cobracket. In [AKKN18b] this enhancement is necessary in order to establish the relationship between the Goldman–Turaev Lie bialgebra and Kashiwara–Vergne theory. To define the enhanced cobracket, a curve in  $|\mathbb{C}\pi|$  is lifted to an immersed curve with a fixed rotation number. Below we review the definitions of the Goldman bracket and the enhanced version of the Turaev cobracket.

The Goldman Bracket sums over smoothing intersections between two free loops. For a free loop  $\alpha$  in  $|\mathbb{C}\pi|$  and a point  $q$  on  $\alpha$ , denote by  $\alpha_q$  the loop  $\alpha$  based at  $q$ .

**def:bracket**

**Definition 3.2** (The Goldman bracket). Let  $\alpha, \beta \in |\mathbb{C}\pi|$  be free loops with homotopy representatives chosen so that there are only finitely many transverse double intersections between  $\alpha$  and  $\beta$ . The Goldman bracket  $[\cdot, \cdot]_G : |\mathbb{C}\pi| \otimes |\mathbb{C}\pi| \rightarrow |\mathbb{C}\pi|$  is given by

$$[\alpha, \beta]_G := - \sum_{q \in \alpha \cap \beta} \varepsilon_q |\alpha_q \beta_q|,$$

where  $\varepsilon_q = \varepsilon(\dot{\alpha}_q, \dot{\beta}_q) \in \{\pm 1\}$  is the local intersection number of  $\alpha$  and  $\beta$  at  $q$ ,  $\alpha_q \beta_q$  is the concatenation of  $\alpha_q$  and  $\beta_q$ , and the extension to  $|\mathbb{C}\pi|$  is linear. Then one easily checks that  $[\cdot, \cdot]_G$  is a Lie bracket on  $|\mathbb{C}\pi|$ .

The original definition of the Turaev cobracket is similar, but uses self intersections of a curve in place of the intersections between two curves. Unfortunately, it is not well-defined with respect to the Reidemeister 1 relation for free homotopy curves, hence the need for the enhancement. We construct the (enhanced) cobracket via a self-intersection map for *based* curves, as in [AKKN18b, Section 5.2]; this definition lends itself well to direct comparison with the three-dimensional

<sup>4</sup>Not to be confused with the abelianisation of  $A$ . In particular,  $|A|$  does not inherit an algebra structure from  $A$ .

The sign here (with the minus sign in front) matches with AKKN genus 0, but is the opposite of AKKN higher genus and Goldman's original definition. Our current multiplication and bracket matches the sign here, so if we change the sign then we should change the stacking order of our multiplication.

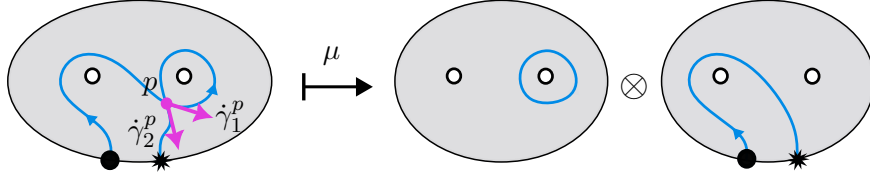


fig: defmu

FIGURE 5. Example of the self intersection map  $\mu$  where  $\epsilon_p = -1$ .

operations of Section 5. For a based curve  $\gamma$  in  $\mathbb{C}\pi$ , the idea is to “snip off” portions of  $\gamma$  at self intersection points to get two curves, one of which is based and the other free. Figure 5 shows an example.

def: mu

**Definition 3.3** (The self-intersection map). For  $\gamma \in \mathbb{C}\pi$ , let  $\tilde{\gamma} \in \mathbb{C}\tilde{\pi}$  denote a path such that  $\tilde{\gamma}\nu$  is homotopic to  $\gamma$ ; and such that  $\tilde{\gamma}$  has only transverse double points, and  $\text{rot}(\tilde{\gamma}) = 1/2$  (hence,  $\text{rot}(\tilde{\gamma}\nu) = 0$ ). Let  $\tilde{\gamma} \cap \tilde{\gamma}$  denote the set of double points. The self intersection map  $\mu$  is defined as follows:

$$\mu : \mathbb{C}\pi \rightarrow |\mathbb{C}\pi| \otimes \mathbb{C}\pi$$

$$\mu(\gamma) = - \sum_{p \in \tilde{\gamma} \cap \tilde{\gamma}} \epsilon_p |\tilde{\gamma}_{t_1^p t_2^p}| \otimes \tilde{\gamma}_{0t_1^p} \tilde{\gamma}_{t_2^p 1},$$

where  $t_1^p$  and  $t_2^p$  are the first and second time parameter in  $[0, 1]$  where  $\tilde{\gamma}$  goes through  $p$ ; where  $\tilde{\gamma}_{rs}$  denotes the path traced by  $\tilde{\gamma}$  from  $t = r$  to  $t = s$ ; the sign  $\epsilon_p = \varepsilon(\dot{\tilde{\gamma}}(t_1^p), \dot{\tilde{\gamma}}(t_2^p)) \in \{\pm 1\}$  is the local self-intersection number; and the formula extends to  $\mathbb{C}\pi$  linearly.

The Turaev cobracket is obtained from  $\mu$  by closing off the path component and making the tensor product alternating: this descends to a map on  $|\mathbb{C}\pi|$ , as follows.

**Definition 3.4** (The Turaev co-bracket). The Turaev cobracket  $\delta$  is the unique linear map which makes the following diagram commute, where  $\text{Alt}(x \otimes y) = x \otimes y - y \otimes x = x \wedge y$ :

$$\begin{array}{ccccc} \mathbb{C}\pi & \xrightarrow{\mu} & |\mathbb{C}\pi| \otimes \mathbb{C}\pi & \xrightarrow{1 \otimes |\cdot|} & |\mathbb{C}\pi| \otimes |\mathbb{C}\pi| \\ \downarrow |\cdot| & & & & \downarrow \text{Alt} \\ |\mathbb{C}\pi| & \xrightarrow{\delta} & & & |\mathbb{C}\pi| \wedge |\mathbb{C}\pi| \end{array}$$

**3.3. Associated graded Goldman-Turaev Lie bialgebra.** There I-adic filtration on  $\mathbb{C}\pi$  is the filtration by powers of the augmentation ideal  $\mathcal{I} = \langle \{\alpha - 1\}_{\alpha \in \pi} \rangle$ :

$$\mathbb{C}\pi = \mathcal{I}^0 \supseteq \mathcal{I} \supseteq \mathcal{I}^2 \supseteq \dots$$

$$\left[ \text{circle with } x, \text{circle with } x \right]_{\text{gr } G} = \sum_{\text{matching pairs}} \text{diagram 1} - \text{diagram 2}$$

FIGURE 6. A schematic diagrammatic example of the graded Goldman bracket.

fig:grbracket

By the 1930's work of Magnus [Mag35], the associated graded algebra of  $\mathbb{C}\pi$  with respect to this filtration is the degree completed free algebra  $\text{FA} = \text{FA}\langle x_1, \dots, x_p \rangle$ :

**Proposition 3.5.** *Given the set of standard generators  $\{\gamma_i\}_{i=1}^p$  for  $\pi$ , there is an isomorphism of algebras  $\text{gr } \mathbb{C}\pi \rightarrow \text{FA}$  and the exponential expansion  $\varphi(\gamma_i^{\pm 1}) = e^{\pm x_i}$  is a homomorphic expansion.*

The I-adic filtration of  $\mathbb{C}\pi$  descends to a filtration on  $|\mathbb{C}\pi|$ :

$$|\mathbb{C}\pi| = |\mathcal{I}^0| \supseteq |\mathcal{I}| \supseteq |\mathcal{I}^2| \supseteq \dots$$

The completed associated graded vector space for  $|\mathbb{C}\pi|$  with respect to this filtration is, by definition

$$\text{gr } |\mathbb{C}\pi| = \prod_{n=0}^{\infty} |\mathcal{I}^n|/|\mathcal{I}^{n+1}|.$$

There is an isomorphism  $\text{gr } |\mathbb{C}\pi| \cong |\text{FA}|$ , where  $|\text{FA}|$  denotes the linear quotient  $|\text{FA}| = \text{FA}/[\text{FA}, \text{FA}]$ , and the exponential expansion descends to a homomorphic expansion for  $|\mathbb{C}\pi|$ . The vector space  $|\text{FA}|$  is spanned by cyclic words in letters  $x_1, \dots, x_p$ , that is, words modulo cyclic permutations of the letters.

Therefore,  $|\text{FA}|$  carries the structure of a Lie bialgebra under  $\text{gr}[\cdot, \cdot]_G$  and  $\text{gr } \delta$  [AKKN18a, Section 3]. Note that the Goldman bracket and the Turaev co-bracket are not strictly filtered maps, as they both shift filtered degree down by one<sup>5</sup>. For example, if  $x \in |\mathcal{I}^r|$  and  $y \in |\mathcal{I}^s|$ , then  $[x, y]_G \in |\mathcal{I}^{r+s-1}|$ . Correspondingly, the associated graded operations are maps of degree  $-1$ .

Figure 6 shows a schematic calculation of the graded Goldman bracket, with cyclic words represented diagrammatically as letters along a circle. The graded Goldman bracket sums over matching pairs of letters in  $z$  and  $w$ , joins the circles at the matching letter, and takes the difference of the two ways of including only one copy of the letter in the new cyclic word. Stated algebraically, this is summarised as follows:

**Proposition 3.6.** [AKKN18a, Section 3.3] *Let  $z = |z_1 \cdots z_l|$  and  $w = |w_1 \cdots w_m|$  be two cyclic words in  $|\text{FA}|$ . The graded Goldman bracket*

$$\text{gr } ([-, -]_G) = [-, -]_{\text{gr } G} : |\text{FA}| \otimes |\text{FA}| \rightarrow |\text{FA}|$$

<sup>5</sup>In [AKKN18a, Sections 3.3, 3.4] the down-shifts are by up to two filtered degrees, as the generating curves around genera and those around boundary components carry different weights. In our genus zero setting this translates to a degree shift of  $-1$ .

prop:gr\_bracket\_def

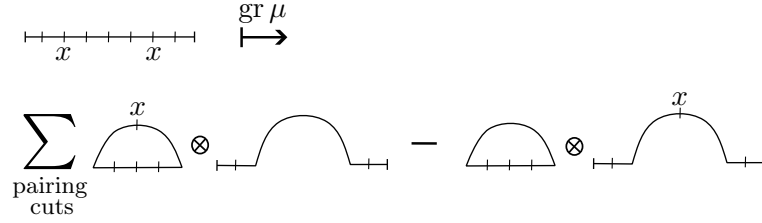


FIGURE 7. A schematic diagrammatic example of the graded Self-intersection map,  $\text{gr } \mu$ .

fig:grmu

is given by:

$$[z, w]_{\text{gr } G} = \sum_{j,k} \delta_{z_j, w_k} (|w_1 \dots w_{k-1} z_{j+1} \dots z_l z_1 \dots z_j w_{k+1} \dots w_m| - |w_1 \dots w_{k-1} z_j \dots z_l z_1 \dots z_{j-1} w_{k+1} \dots w_m|),$$

where  $\delta_{z_j, w_k}$  is the Kronecker delta.

Figure 7 shows a schematic diagrammatic calculation of the graded self-intersection map  $\mu$ , as a sum over *pairing cuts*. A pairing cut identifies two matching letters in a word, and splits the word along a chord connecting these matching letters. The graded self-intersection map outputs the tensor product of the resulting cyclic word and the remainder of the associative word. In formulas:

**Proposition 3.7.** [AKKN18a, Section 3.4] Let  $w = w_1 \dots w_m \in \text{As}_p$ . The graded self-intersection map

$$\text{gr}(\mu) = \mu_{\text{gr}} : \text{FA} \rightarrow |\text{FA}| \otimes \text{FA}$$

is given by:

$$\mu_{\text{gr}}(w) = \sum_{j < k} \delta_{w_j, w_k} (|w_j \dots w_{k-1}| \otimes w_1 \dots w_{j-1} w_{k+1} \dots w_m - |w_{j+1} \dots w_{k-1}| \otimes w_1 \dots w_j w_{k+1} \dots w_m),$$

where  $\delta_{w_j, w_k}$  denotes the Kronecker delta.

Figure 8(A.) shows a schematic diagrammatic definition of the graded Turaev co-bracket, again as a sum over *pairing cuts*. A pairing cut in a cyclic word identifies a pair of coinciding letters, and cuts the cycle into two cycles along the chord connecting the matching letters. To obtain the cobracket, one takes a sum of wedge products of the resulting split cyclic words, adding one copy of the coinciding letter to either side, as shown in Figure 8(B.) and expressed in formulas below:

**Proposition 3.8.** [AKKN18a, Section 3.4] Let  $w = w_1 \dots w_m \in |\text{As}_p|$ . The graded Turaev cobracket

$$\text{gr}(\delta) = \delta_{\text{gr}} : |\text{FA}| \rightarrow |\text{FA}| \wedge |\text{FA}|$$

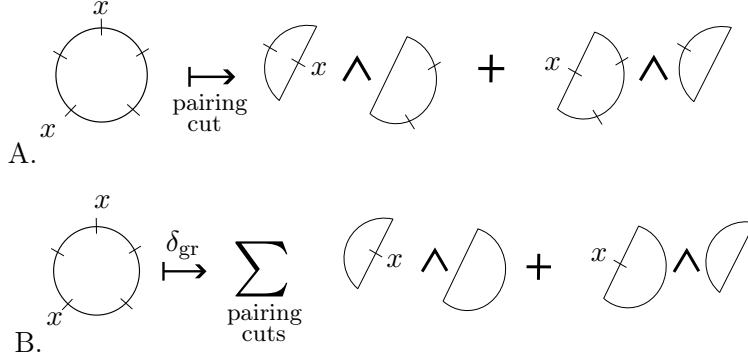


FIGURE 8. (A.) An example pairing cut of a cyclic word. (B.) An example of the graded Turaev cobracket as a sum over pairing cuts of a cyclic word.

fig:paircut

is given by

$$\delta_{\text{gr}}(w) = \sum_{j < k} \delta_{w_j, w_k} (|w_j \dots w_{k-1}| \wedge |w_{k+1} \dots w_m w_1 \dots w_{j-1}| + |w_k \dots w_m w_1 \dots w_{j-1}| \wedge |w_{j+1} \dots w_{k-1}|),$$

where  $\delta_{w_j, w_k}$  denotes the Kronecker delta<sup>6</sup>.

#### 4. EXPANSIONS FOR TANGLES IN HANDLEBODIES

**4.1. Framed oriented tangles.** This section introduces the space  $\mathbb{C}\tilde{\mathcal{T}}$  of framed, oriented tangles in a genus  $p$  handlebody, with formal linear combinations. Our main result – proven in Section 5 – is that homomorphic expansions on  $\mathbb{C}\tilde{\mathcal{T}}$  induce homomorphic expansions on the Goldman-Turaev Lie biagebra.

Let  $M_p$  denote the manifold  $D_p \times I$  where  $D_p$  is a disc in the complex plane with  $p$  points removed. While  $M_p$  is not a compact manifold, knot theory in  $M_p$  is equivalent to knot theory in a genus  $p$  handlebody. For the purpose of the Kontsevich integral, we identify  $D_p$  with a unit square  $[0, 1] + [0, i]$  in the complex plane with  $p$  points removed, so  $M_p$  can be drawn as a cube with  $p$  vertical lines removed; we call these lines *poles*, as shown in the middle in Figure 9. We refer to  $D_p \times \{0\}$  as the “floor” or “bottom”, and  $D_p \times \{1\}$  as the “ceiling” or “top”. The “back wall” is the face  $[i, i + 1] \times [0, 1]$ . We refer to the  $i \in \mathbb{C}$  direction as North.

def:tangle

**Definition 4.1.** An oriented tangle  $T$  in  $M_p$  is an embedding of an oriented compact 1-manifold

$$(S, \partial S) \hookrightarrow (M_p, D_p \times \{0\} \cup D_p \times \{1\}).$$

<sup>6</sup>Apologies for the notation clash.



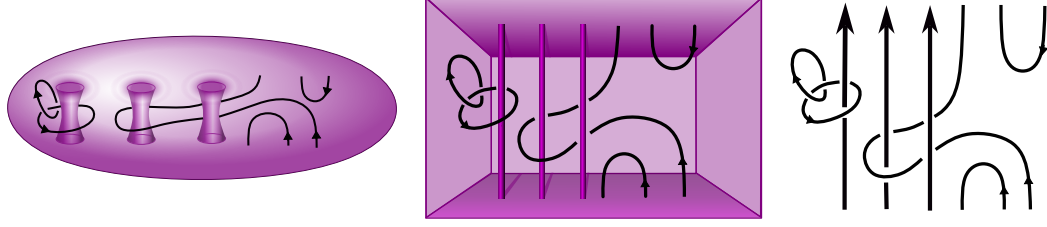


FIGURE 9. An example of a tangle in  $M_3$ , drawn first in a handlebody, then in a cube with poles, and lastly as a tangle diagram projected to the back wall of the cube.

fig:polestudio

The interior of  $S$  lies in the interior of  $M_p$ , and the boundary points of  $S$  are mapped to the top or bottom. Oriented tangles in  $M_p$  are considered up to ambient isotopy fixing the boundary. We denote the set of isotopy classes by  $\mathcal{T}$ . An example is shown in Figure 9.

**Definition 4.2.** A *framing* for an oriented tangle  $T$  in  $M_p$  is a continuous choice of unit normal vector at each point of  $T$ , which is fixed pointing North at the boundary points. *Framed oriented tangles* in  $M_p$  are also considered up to ambient isotopy fixing the boundary. We denote the set of isotopy classes of framed oriented tangles by  $\tilde{\mathcal{T}}$ .

Henceforth, any tangle is assumed to be framed and oriented unless otherwise stated. The skeleton of a tangle is the underlying combinatorial information with the topology forgotten:

def:skeleton

**Definition 4.3.** The *skeleton*  $\sigma(T)$  of a tangle  $T = (S \hookrightarrow M_p)$  – see Figure 10 – is the set of tangle endpoints  $P_{\text{bot}} \subseteq D_p \times \{0\}$  and  $P_{\text{top}} \subseteq D_p \times \{1\}$ , along with

- (1) A partition of  $P_{\text{bot}} \cup P_{\text{top}}$  into ordered pairs given by the oriented intervals of  $S$ .
- (2) A non-negative integer  $k$ : the number of circles in  $S$ .

The skeleton of a framed tangle is the same as the skeleton of the underlying unframed tangle. The set of framed tangles in  $M_p$  with skeleton  $S$  is denoted  $\tilde{\mathcal{T}}(S)$ . For example,  $\tilde{\mathcal{T}}(\bigcirc)$  is the set of framed knots in  $M_p$ .

The linear extension of  $\tilde{\mathcal{T}}(S)$ , denoted  $\mathbb{C}\tilde{\mathcal{T}}(S)$ , is the vector space of  $\mathbb{C}$ -linear combinations of tangles in  $\tilde{\mathcal{T}}(S)$ . We denote by  $\mathbb{C}\tilde{\mathcal{T}}$  the disjoint union  $\sqcup_S \mathbb{C}\tilde{\mathcal{T}}(S)$  over all skeleta  $S$ . Tangles with different skeleta cannot be linearly combined.

One may represent tangles in  $M_p$  using tangle diagrams in (at least) two different ways: by projecting to the back wall of  $M_p$  or to the floor.

Projecting to the back wall, an  $\ell$ -component tangle in  $M_p$  can be diagrammatically represented as a tangle diagram with  $p$  straight vertical *poles*, and  $\ell$  *tangle strands* of circle and interval components. The strands pass over (in front of) and

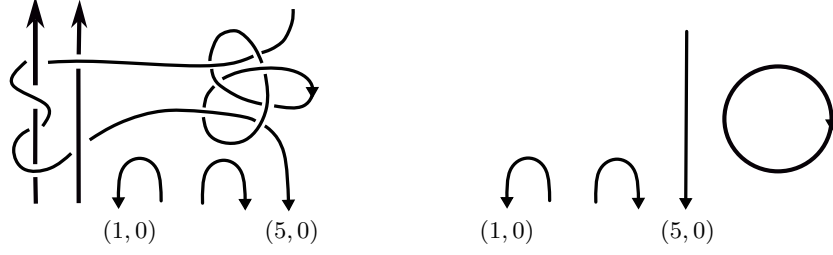


FIGURE 10. On the left is a tangle in  $M_2$ , and on the right is schematic diagram of the skeleton of the tangle. The skeleton of the tangle is the combinatorial data given by the following set of order pairs and the integer 1:  $\{[(2,0),0], [(1,0),0)], [(3,0),0], [(4,0),0)], [(5,0),1], [(5,0),0)], 1\}$

fig:skeleton

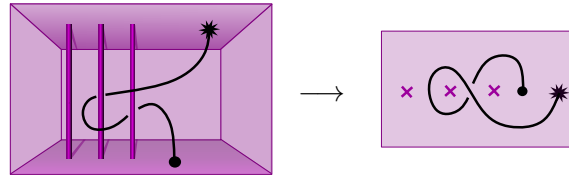


FIGURE 11. An example of a tangle in  $M_3$  projected to the bottom floor of the cube. Strands of a tangle diagram can pass over bottom endpoints (dot) or under top endpoints (star).

fig:BottomDiagram

under (behind) the poles and other strands, as shown on the right in Figure 9. The poles are oriented upwards. By Reidemeister's theorem,  $\tilde{\mathcal{T}}$  is in bijection with such diagrams modulo the Reidemeister moves R2 and R3, and the framed version of R1.

By projecting instead to the floor  $D_p \times \{0\}$ , a tangle in  $M_p$  is represented by a tangle diagram in  $D_p$ . The R2 and R3 moves continue to apply. The endpoints of the tangle are fixed: bottom endpoints are denoted by dots, top endpoints are denoted by stars. Strands of the tangle diagram can pass over bottom endpoints, or under top endpoints, as shown in Figure 11. However, the strands cannot pass across the punctures in  $D_p$ .

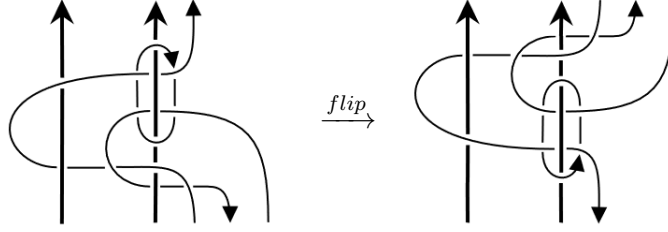
FIGURE 12. A tangle in  $M_2$  and its flip

fig:flip

sec:opsonT

4.2. **Operations on  $\tilde{\mathcal{T}}$ .** There are several useful operations defined on  $\tilde{\mathcal{T}}$ . These operations extend linearly to  $\mathbb{C}\tilde{\mathcal{T}}$ , and are used in Section 5 to relate quotients of  $\mathbb{C}\tilde{\mathcal{T}}$  to the Goldman-Turaev Lie bialgebra.

- *Stacking product:* Given tangles  $T_1, T_2 \in M_p$ , if the top endpoints of  $\sigma(T_1)$  coincide with the bottom endpoints of  $\sigma(T_2)$  in  $D_p$ , and the orientations on the strands of  $T_1$  and  $T_2$  agree, then the product  $T_1 T_2$  is the tangle obtained by stacking  $T_2$  on top of  $T_1$ .
- *Strand addition:* The *strand addition* operation adds a non-interacting additional strand to a tangle  $T$  at a point  $q \in D_p$  to get a new tangle  $T \sqcup_q \uparrow$ . More precisely, pick a contractible  $U \subseteq D_p$  such that  $T$  is contained entirely in  $U \times [0, 1]$  and a point  $q \in D_p$  outside of  $U$ . The tangle  $T \sqcup_q \uparrow$  is  $T$  together with an upward-oriented vertical strand  $q \times I$  at  $q$ .
- *Strand orientation switch:* This operation reverses the orientation of a given strand of the tangle.
- *Flip:* Given a tangle  $T$  in  $M_p$ , the flip of a tangle  $T$  in  $M_p$ , denoted  $\bar{T}$ , is the mirror image of  $T$  with respect to the ceiling, as shown in Figure 12. When  $T$  is flipped, each top boundary point  $(q, 1)$  becomes a bottom boundary point  $(q, 0)$ , and vice versa. The orientations and framing of the strands of  $T$  are reflected along with the strands. However, the orientations of the poles remain ascending. Equivalently, the flip operation can be defined as reversing the parametrisation of  $I$  in  $M_p \cong D_p \times I$ . This, in effect, flips the orientation of the poles but changes nothing else.

In Section 5.1, we show that the stacking commutator of tangles, given by  $[T_1, T_2] = T_1 T_2 - T_2 T_1$ , induces to the Goldman bracket in the sense of Section 2. In Section 5.2 a similar but more subtle argument relates the flip operation to the Turaev cobracket.

sec:t-filtration

4.3. **The  $t$ -filtration on  $\tilde{\mathcal{T}}$  and the associated graded  $\tilde{\mathcal{A}}$ .** In setting up a theory of Vassiliev invariants for  $\tilde{\mathcal{T}}$ , there are different filtrations to consider. In line with classical notation of Vassiliev invariants, we denote by a double point

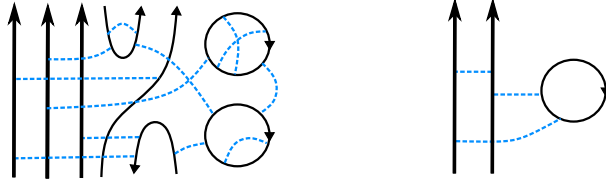


FIGURE 13. Two chord diagrams: an admissible one (left), and a non-admissible one (right) that does contain a pole-pole chord.

ssibleNonAdmissible

the difference between an over-crossing and an under-crossing:

$$\times = \nearrow \searrow - \searrow \nearrow.$$

Double points, however, come in two varieties: *pole-strand*, if the crossing occurs between a pole and a tangle strand, and *strand-strand*, if the crossing occurs between two tangle strands. As the poles are fixed, they never cross each other, hence, there are no pole-pole double points.

The main filtration we consider on  $\mathbb{C}\tilde{\mathcal{T}}$  is the filtration by the total number of double points of either type, as well as strand framing changes (as in Section 3.1). We call this the *total filtration*, or *t-filtration* for short, and write it as

$$\mathbb{C}\tilde{\mathcal{T}} = \tilde{\mathcal{T}}_0 \supseteq \tilde{\mathcal{T}}_1 \supseteq \tilde{\mathcal{T}}_2 \supseteq \tilde{\mathcal{T}}_3 \supseteq \cdots$$

where  $\tilde{\mathcal{T}}_t$  is the set of linear combinations of framed tangle diagrams with at least  $t$  total double points and strand framing changes. In spirit, this filtration comes from the diagrammatic view of projecting to the back wall of the cube.

The associated graded space of  $\mathbb{C}\tilde{\mathcal{T}}$  with respect to the total filtration is

$$\tilde{\mathcal{A}} := \text{gr } \mathbb{C}\tilde{\mathcal{T}} = \prod_{t \geq 0} \tilde{\mathcal{T}}_t / \tilde{\mathcal{T}}_{t+1}.$$

The degree  $t$  component of  $\tilde{\mathcal{A}}$  is  $\tilde{\mathcal{A}}_t := \tilde{\mathcal{T}}_t / \tilde{\mathcal{T}}_{t+1}$ .

As in classical Vassiliev theory (cf. section 3.1), the associated graded space  $\tilde{\mathcal{A}}$  has a combinatorial description in terms of *chord diagrams*.

**Definition 4.4.** A *chord diagram* on a tangle skeleton is an even number of marked points on the poles and skeleton strands, up to orientation preserving diffeomorphism, along with a perfect matching on the marked points – that is, a partition of marked points into unordered pairs. In diagrams, the pairs are connected by a *chord*, indicated by a dashed line, as in Figure 13.

def:admissible

**Definition 4.5.** A chord diagram is *admissible* if all chords connect strands to strands, or strands to poles, but there are no pole-pole chords. See Figure 13 for examples.

def:cdspace

**Definition 4.6.** The space  $\mathcal{D}(S)$  of *admissible chord diagrams on a skeleton*  $S$  is the space of  $\mathbb{C}$ -linear combinations of admissible chord diagrams on the skeleton

Dror thinks we should  
remove the last sentence

$$\text{Diagram 1} + \text{Diagram 2} - \text{Diagram 3} - \text{Diagram 4} = 0$$

FIGURE 14. The 4T relation, which is admissible if at most one of the three skeleton components is a pole.

fig:Admissible 4T

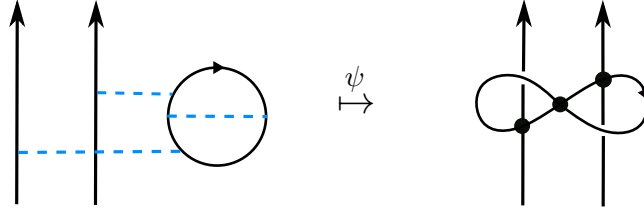


FIGURE 15. Example of  $\psi$  with the right hand side viewed as an element of  $\tilde{\mathcal{T}}_3/\tilde{\mathcal{T}}_4$ . Different choices of over or under crossings with the poles only differ by elements of  $\tilde{\mathcal{T}}_4$ .

fig:psi

$S$ , modulo *admissible* 4T relations, shown in Figure 14. Admissible 4T relations are 4T relations where all four terms are admissible<sup>7</sup>. That is,

$$\mathcal{D}(S) = \frac{\mathbb{C}\langle \text{admissible chord diagrams on } S \rangle}{\{\text{admissible 4T relations}\}}$$

The space  $\mathcal{D}(S)$  is a graded vector space, where the degree is given by the number of chords. Denote the degree  $t$  component of  $\mathcal{D}(S)$  by  $\mathcal{D}_t(S)$ . Let  $\mathcal{D}$  denote the disjoint union  $\sqcup_S \mathcal{D}(S)$ , and denote the degree  $t$  component of  $\mathcal{D}$  by  $\mathcal{D}_t = \sqcup_S \mathcal{D}_t(S)$ .

The well-known map  $\psi : \mathcal{D} \rightarrow \tilde{\mathcal{A}}$  from classical Vassiliev theory is defined as follows. In degree  $t$ ,  $\psi_t : \mathcal{D}_t \rightarrow \tilde{\mathcal{T}}_t/\tilde{\mathcal{T}}_{t+1}$ , “contracts” the  $t$  chords to double points, as shown in Figure 15. This may create other crossings, but modulo  $\tilde{\mathcal{T}}_{t+1}$  the over/under information at these crossings does not matter.

**Lemma 4.7.** *The map  $\psi$  is well-defined and surjective.*

*Proof.* To show  $\psi$  is well-defined, it suffices to show that admissible 4T relations in  $\mathcal{D}_t$  are in the kernel of  $\psi$ . This is the standard “lasso trick” recalled in Figure 16. For surjectivity, recall from Section 3.1.2 that a framing change in  $\tilde{\mathcal{A}}$  is half of chord. So, both framing changes and double points are in the image of  $\psi$ , and thus  $\psi$  is surjective.  $\square$

citation needed

<sup>7</sup>Equivalently, a 4T relation is admissible if at most one of the three skeleton components involved is a pole.

$$\psi \left( - \begin{array}{c} \uparrow \uparrow \uparrow \uparrow \\ \text{---} \text{---} \text{---} \text{---} \end{array} + \begin{array}{c} \uparrow \uparrow \uparrow \uparrow \\ \text{---} \text{---} \text{---} \end{array} + \begin{array}{c} \uparrow \uparrow \uparrow \uparrow \\ \text{---} \text{---} \end{array} - \begin{array}{c} \uparrow \uparrow \uparrow \uparrow \\ \text{---} \text{---} \end{array} \right) = - \begin{array}{c} \uparrow \\ \text{---} \end{array} + \begin{array}{c} \uparrow \\ \text{---} \end{array} + \begin{array}{c} \uparrow \\ \text{---} \end{array} - \begin{array}{c} \uparrow \\ \text{---} \end{array} = \begin{array}{c} \uparrow \\ \text{---} \end{array} - \begin{array}{c} \uparrow \\ \text{---} \end{array} = 0$$

FIGURE 16. Showing that  $\psi : \mathcal{D} \rightarrow \tilde{\mathcal{A}}$  is well defined. The figure is understood locally: in degree  $t$  the chord diagrams have  $t - 2$  other chords elsewhere, and correspondingly the tangles have  $t - 2$  other double points elsewhere.

fig:psicomputation

According to Lemma 3.1, in order to show that  $\psi$  is an isomorphism, one needs to find an expansion valued in  $\mathcal{D}$ .

thm:Zwelldefined

**Lemma 4.8.** *The framed Kontsevich integral  $Z : \mathbb{C}\tilde{\mathcal{T}} \rightarrow \mathcal{D}$  satisfies the conditions of Lemma 3.1: it is filtered, and  $\psi \circ \text{gr } Z = \text{id}_{\tilde{\mathcal{A}}}$ .*

*Proof.* This is a variant of a standard fact [Kon93]; one detailed explanation is in [BN95, Section 4.3]. A small point to verify is that the image of  $Z$  on an element of  $\mathbb{C}\tilde{\mathcal{T}}$  is an admissible chord diagram. This is immediate from the definition of the Kontsevich integral: the poles are parallel, hence the coefficient of a chord diagram with a pole-pole chord is computed by integrating zero. The main part, that  $\psi \circ \text{gr } Z = \text{id}_{\tilde{\mathcal{A}}}$ , is done as in [BN95, Section 4.4.2, Thm 1 part (3)].  $\square$

The next corollary is then immediate from Lemma 3.1:

cor:grcd

**Corollary 4.9.** *The map  $\psi : \mathcal{D} \rightarrow \tilde{\mathcal{A}}$  is an isomorphism, and  $Z$  is an expansion for  $\tilde{\mathcal{T}}$ .*

For a skeleton  $S$ , we denote by  $\tilde{\mathcal{A}}(S)$  the space of admissible chord diagrams on the skeleton  $S$ , so  $\tilde{\mathcal{A}}(S)$  is the associated graded vector space of  $\mathbb{C}\tilde{\mathcal{T}}(S)$ . For example,  $\tilde{\mathcal{A}}(\bigcirc)$  is the associated graded vector space of the space of knots in  $M_p$ .

**4.4. Operations on  $\tilde{\mathcal{A}}$ .** The tangle operations *stacking*, *strand addition*, *strand orientation switch*, and *flip* on  $\tilde{\mathcal{T}}$  induce associated graded operations by the same names on  $\tilde{\mathcal{A}}$ . In view of Corollary 4.9, we give descriptions of these operations using chord diagrams.

The operation *stacking* is given by concatenating the skeleta of two chord diagrams (as long as they have the same number of poles, and the top endpoints of one match the bottom endpoints of the other, including orientations).

The associated graded *strand addition* operation adds a vertical skeleton strand to a chord diagram. The new strand has no chord endings.

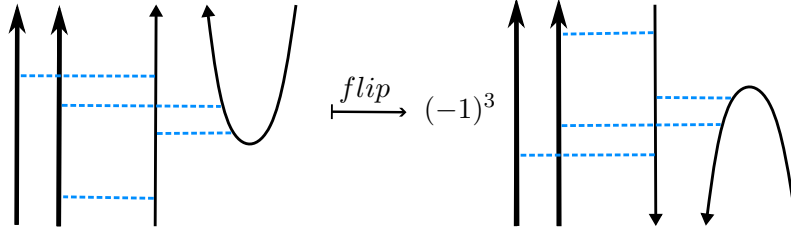


FIGURE 17. An example chord diagram and its flip.

chorddiagoperations

The associated graded *strand orientation switch* for strand  $e$  switches the orientation of the strand  $e$ , and multiplies each chord diagram with  $(-1)$  to the power of the number of chord endings on  $e$ . The sign arises from the fact that reversing the orientation of  $e$  changes the signs of double points between  $e$  and any other distinct strand or pole.

The associated graded operation *flip* reflects a chord diagram with respect to a “mirror on the ceiling”; then reverses the orientations of the poles so that they are oriented upwards, as in see Figure 17; and multiplies by a factor of  $(-1)^m$ , where  $m$  is the total number of chord endings on the poles. The factor of  $(-1)^m$  arises from the pole orientation reversals, as this changes the signs of any pole-strand double points. 17.

The following proposition is straightforward from the definition of  $Z$ .

prop:Zhomom

**Proposition 4.10.** *The Kontsevich integral  $Z$  intertwines stacking, strand additions, orientation reversals and flips with their associated graded operations.*  $\square$

sec:s-sfiltration

**4.5. The  $s$ -filtration on  $\tilde{\mathcal{T}}$  and  $\tilde{\mathcal{A}}$ .** Recall from Section 4.3 that the total filtration on  $\mathbb{C}\tilde{\mathcal{T}}$  is given by strand framing changes and double points between strands with poles and strands with strands. In this section we introduce a second filtration on  $\mathbb{C}\tilde{\mathcal{T}}$ , given by strand framing changes, and *only strand-strand* double points. We call this the *strand filtration*, or simply *s-filtration*.

We use subscripts for the  $s$ -filtration:

$$\mathbb{C}\tilde{\mathcal{T}} = \tilde{\mathcal{T}}^0 \supseteq \tilde{\mathcal{T}}^1 \supseteq \tilde{\mathcal{T}}^2 \supseteq \tilde{\mathcal{T}}^3 \supseteq \dots,$$

where  $\tilde{\mathcal{T}}^s \subseteq \mathbb{C}\tilde{\mathcal{T}}$  is spanned by tangles with at least  $s$  strand framing changes or strand double points.

*Remark 4.11.* The associated graded structure of  $\mathbb{C}\tilde{\mathcal{T}}$  with respect to the  $s$ -filtration was studied by Habiro and Massuyeau in [HM21], as part of their work on *bottom tangles*<sup>8</sup>. Yet we do not apply the associated graded functor to the  $s$ -filtration, but rather, quotient only by  $\tilde{\mathcal{T}}^1$  and  $\tilde{\mathcal{T}}^2$  to identify the Goldman-Turaev spaces and operations in Section 5.

<sup>8</sup>Projecting to the bottom of the cube rather than the back wall makes the strand filtration the natural Vassiliev filtration to consider.

In turn, the  $s$ -filtration induces a filtration on  $\tilde{\mathcal{A}}$ , as follows. Let  $\tilde{\mathcal{T}}_t^s$  denote  $\tilde{\mathcal{T}}_t \cap \tilde{\mathcal{T}}^s$ : that is, the linear span of tangles in  $\mathbb{C}\tilde{\mathcal{T}}$ , which that have at least  $t$  double points or framing changes, at least  $s$  of which are strand-strand double points or framing changes.

ionQuotientNotation

**Definition 4.12.** Denote by  $\tilde{\mathcal{A}}^{\geq s}$  the  $s$ -filtered component of  $\tilde{\mathcal{A}}$ :

$$\tilde{\mathcal{A}}^{\geq s} := \prod \tilde{\mathcal{T}}_t^s / \tilde{\mathcal{T}}_{t+1}^s.$$

Explicitly,  $\tilde{\mathcal{A}}^{\geq s}$  is spanned by chord diagrams with at least  $s$  strand-strand chords.

For strand-strand chords we will use the shorthand word  $s$ -chords. Note that the number of  $s$ -chords is only a filtration, not itself grading on  $\tilde{\mathcal{A}}$ , as the 4T relation is not homogeneous with respect to the number of  $s$ -chords.

prop:ZrespectsS

**Proposition 4.13.** *The Kontsevich integral  $Z$  is a filtered map with respect to the  $s$ -filtration.*

*Proof.* This is a close analogue of Theorem 4.8. As strand-strand double points correspond to strand-strand chords via the identification  $\psi$  of the associated graded space with chord diagrams, the proof translates verbatim from [BN95, Section 4.3].  $\square$

sec:Conway

**4.6. The Conway quotient.** In this section we introduce the last necessary ingredient for identifying the Goldman-Turaev operations: the Conway quotient of  $\mathbb{C}\tilde{\mathcal{T}}$ . This is essentially the Conway skein module of tangles in  $M_p$ , but without fixing the value of the unknot. We show that the Kontsevich integral descends to the Conway quotient.

**Definition 4.14.** The Conway quotient of  $\mathbb{C}\tilde{\mathcal{T}}$ , denoted  $\mathbb{C}\tilde{\mathcal{T}}_{\nabla}$ , is given by

$$\mathbb{C}\tilde{\mathcal{T}}_{\nabla} := \mathbb{C}\tilde{\mathcal{T}}[[a]] \Big/ \left( \text{strand-strand crossing} - \text{strand-strand crossing} = (e^{\frac{a}{2}} - e^{-\frac{a}{2}}) \text{cup} \right),$$

where  $a$  is a formal variable of  $t$  and  $s$  degree 1, and the skein relation is restricted to strand-strand crossings. We use the shorthand  $b := e^{\frac{a}{2}} - e^{-\frac{a}{2}}$ .

The  $t$  and  $s$  filtrations on  $\mathbb{C}\tilde{\mathcal{T}}$  induce filtrations on  $\mathbb{C}\tilde{\mathcal{T}}_{\nabla}$ . Let  $\tilde{\mathcal{T}}_{\nabla,t}$  denote the  $t$ -filtered component in the total filtration of  $\mathbb{C}\tilde{\mathcal{T}}_{\nabla}$ , and  $\tilde{\mathcal{A}}_{\nabla} := \text{gr}_t \mathbb{C}\tilde{\mathcal{T}}_{\nabla} = \prod \tilde{\mathcal{T}}_{\nabla,t} / \tilde{\mathcal{T}}_{\nabla,t+1}$  denote the associated graded algebra of  $\mathbb{C}\tilde{\mathcal{T}}_{\nabla}$  with respect the total filtration. We now show that  $\tilde{\mathcal{A}}_{\nabla}$  has a chord diagrammatic description similar to Corollary 4.9. Recall that  $\mathcal{D}$  is the space of chord diagrams on tangle skeleta, modulo admissible 4T relations.

**Definition 4.15.** The conway quotient of  $\mathcal{D}$  is given by

$$\mathcal{D}_{\nabla} := \mathcal{D}[[a]] \Big/ \left( \text{cup} = a \text{cup}, \text{cup} = a \text{cup} \right)$$

where the new relations are restricted to chords on strand skeleton components (not poles).



Note that the two new relations in  $\mathcal{D}_\nabla$  are equivalent, shown in both combinations of orientations for convenience. Furthermore, the relations are homogeneous (respect the  $t$ -grading) on  $\mathcal{D}$ , and therefore  $\mathcal{D}_\nabla$  is also graded by the sum of the total number of chords and the exponent of  $a$ . The next theorem shows that  $\tilde{\mathcal{A}}_\nabla \cong \mathcal{D}_\nabla$ : this essentially follows from the results of [LM95]. For completeness we present a direct proof.

thm:Z\_conway

**Theorem 4.16.** *The isomorphism  $\psi$  descends to an isomorphism  $\psi_\nabla : \tilde{\mathcal{A}}_\nabla \cong \mathcal{D}_\nabla$ , and the Kontsevich integral descends to an expansion  $Z_\nabla : \mathbb{C}\tilde{\mathcal{T}}_\nabla \rightarrow \mathcal{D}_\nabla$ .*

*Proof.* First we show that  $\psi$  descends to a surjective graded map  $\psi : \mathcal{D}_\nabla \rightarrow \tilde{\mathcal{A}}_\nabla$ . To show that  $\psi$  is well-defined, we need to show that the Conway relations in  $\mathcal{D}_\nabla$  is in the kernel. We verify one of the two equivalent relations:

$$\psi \left( \updownarrow - a \begin{array}{c} \nearrow \searrow \\ \nwarrow \nearrow \end{array} \right) = \updownarrow - a \begin{array}{c} \nearrow \searrow \\ \nwarrow \nearrow \end{array} = a \begin{array}{c} \nearrow \searrow \\ \nwarrow \nearrow \end{array} - a \begin{array}{c} \nearrow \searrow \\ \nwarrow \nearrow \end{array} = 0.$$

Next, we verify that the Kontsevich integral  $Z$  descends to a map  $\mathbb{C}\tilde{\mathcal{T}}_\nabla \rightarrow \tilde{\mathcal{A}}_\nabla$  by verifying the relations in  $\mathbb{C}\tilde{\mathcal{T}}_\nabla$ . We do this first at the level of tangles with two bottom and two top endpoints (directly above). Recall that the Kontsevich integral is invariant under both total horizontal and total vertical rescaling, and hence well-defined for such two-two tangles without specifying the distance between the endpoints.

Recall that

$$Z(\begin{array}{c} \nearrow \searrow \\ \nwarrow \nearrow \end{array}) = \left( e^{\frac{C}{2}} \right) \cdot \begin{array}{c} \nearrow \searrow \\ \nwarrow \nearrow \end{array}, \quad \text{and} \quad Z(\begin{array}{c} \nwarrow \nearrow \\ \nearrow \searrow \end{array}) = \left( e^{-\frac{C}{2}} \right) \cdot \begin{array}{c} \nwarrow \nearrow \\ \nearrow \searrow \end{array},$$

where  $C$  denotes a chord, the exponential is interpreted formally as a power series with the stacking multiplication, as shown in the first equality below. Using the Conway relation, we compute:

$$C^k = \left\{ \begin{array}{c} \uparrow \uparrow \\ \text{---} \\ \uparrow \uparrow \end{array} \right\}_k \stackrel{\nabla}{=} a^k \left\{ \begin{array}{c} \nearrow \searrow \\ \nwarrow \nearrow \\ \text{---} \\ \nearrow \searrow \\ \nwarrow \nearrow \end{array} \right\}_k = a^k (\begin{array}{c} \nearrow \searrow \\ \nwarrow \nearrow \end{array})^k = \begin{cases} a^k \uparrow \uparrow, & \text{if } k \text{ is even} \\ a^k \begin{array}{c} \nearrow \searrow \\ \nwarrow \nearrow \end{array}, & \text{if } k \text{ is odd} \end{cases}$$

Now applying  $Z$  to the left hand side of the Conway relation, we obtain

$$\begin{aligned} Z(\begin{array}{c} \nearrow \searrow \\ \nwarrow \nearrow \end{array}) - Z(\begin{array}{c} \nwarrow \nearrow \\ \nearrow \searrow \end{array}) &= (e^{\frac{C}{2}} - e^{-\frac{C}{2}}) \begin{array}{c} \nearrow \searrow \\ \nwarrow \nearrow \end{array} \\ &= \sum_{k=0}^{\infty} \left( \frac{C^k}{2^k k!} - \frac{(-1)^k C^k}{2^k k!} \right) \begin{array}{c} \nearrow \searrow \\ \nwarrow \nearrow \end{array} = \sum_{k=0}^{\infty} \frac{C^{2k+1}}{2^{2k} (2k+1)!} \begin{array}{c} \nearrow \searrow \\ \nwarrow \nearrow \end{array} \\ &= \sum_{k=0}^{\infty} \frac{a^{2k+1} \begin{array}{c} \nearrow \searrow \\ \nwarrow \nearrow \end{array}}{2^{2k} (2k+1)!} \begin{array}{c} \nearrow \searrow \\ \nwarrow \nearrow \end{array} = \sum_{k=0}^{\infty} \frac{a^{2k+1}}{2^{2k} (2k+1)!} \uparrow \uparrow \\ &= (e^{\frac{a}{2}} - e^{-\frac{a}{2}}) \uparrow \uparrow \\ &= Z \left( (e^{\frac{a}{2}} - e^{-\frac{a}{2}}) \begin{array}{c} \updownarrow \end{array} \right). \end{aligned}$$

$$\begin{array}{c}
\text{Diagram 1} = b \cdot (\text{Diagram 2}) = \text{Diagram 3} \\
\cap \qquad \qquad \qquad \cap \\
\mathbb{C}\tilde{\mathcal{T}}_{\nabla}(\bigcirc\bigcirc\bigcirc\bigcirc) \qquad \qquad \in \mathbb{C}\tilde{\mathcal{T}}_{\nabla}(\bigcirc)
\end{array}$$

FIGURE 18. The map *iota* is not injective: The left hand side and the right hand side are both elements of  $\mathbb{C}\tilde{\mathcal{T}}$ , and equal in  $\mathbb{C}\tilde{\mathcal{T}}_{\nabla}$ . Skeleta in the Conway quotient are not a partition.

fig:ConwaySkel

To see that the local verification above is sufficient, one needs to recall more about the Kontsevich integral. Namely,  $Z$  is multiplicative with respect to the stacking composition of tangles (with fixed endpoints), and asymptotically commutes with “distant disjoint unions”, and these two facts imply the global equality (in fact, they lead to a combinatorial construction of  $Z$  for *parenthesised* tangles). For details see [CDM12, Chapter 8].

Therefore, by Lemma 3.1,  $Z$  is a (homomorphic) expansion for  $\mathbb{C}\tilde{\mathcal{T}}_{\nabla}$  and  $\psi : \mathcal{D}_{\nabla} \rightarrow \tilde{\mathcal{A}}_{\nabla}$  is an isomorphism.  $\square$

Let  $\iota$  denote the composition of the natural embedding with the Conway quotient map

$$\iota : \mathbb{C}\tilde{\mathcal{T}} \rightarrow \mathbb{C}\tilde{\mathcal{T}}[[a]] \rightarrow \mathbb{C}\tilde{\mathcal{T}}_{\nabla}.$$

The map  $\iota$  is not injective, see for example Figure fig:ConwaySkel. However, it is surjective: all  $\mathbb{C}$ -linear combinations of tangles are in the image, and given a tangle  $T$ ,  $b^k T$  is equal in  $\mathbb{C}\tilde{\mathcal{T}}_{\nabla}$  to a tangle with  $k$  double points, which is, in turn, a  $\mathbb{C}$ -linear combination of tangles.

**Definition 4.17.** For skeleton  $S$ , let  $\mathbb{C}\tilde{\mathcal{T}}_{\nabla}(S)$  denote the image  $\iota(\mathbb{C}\tilde{\mathcal{T}}(S))$ .

Note that while the skeleton fibration of  $\mathbb{C}\tilde{\mathcal{T}}$  is a partition into disjoint fibers  $\mathbb{C}\tilde{\mathcal{T}}(S)$ , this is no longer true in  $\mathbb{C}\tilde{\mathcal{T}}_{\nabla}$  due to the non-injectivity of  $\iota$ . For example, the middle term of the equality in Figure 18 lies in both  $\mathbb{C}\tilde{\mathcal{T}}_{\nabla}(\bigcirc)$  and  $\mathbb{C}\tilde{\mathcal{T}}_{\nabla}(\bigcirc\bigcirc\bigcirc\bigcirc)$ .

We will identify the Goldman-Turaev Lie bialgebra in low-degree quotients of the  $s$ -filtration of  $\mathbb{C}\tilde{\mathcal{T}}_{\nabla}$ . The next few propositions establish the necessary understanding of these quotients. Denote by  $\tilde{\mathcal{T}}^{/n}$  the quotient  $\tilde{\mathcal{T}}/\tilde{\mathcal{T}}^n$ , and similarly for the Conway quotients,  $\tilde{\mathcal{T}}_{\nabla}^{/n}$  denotes  $\mathbb{C}\tilde{\mathcal{T}}_{\nabla}/\tilde{\mathcal{T}}_{\nabla}^n$ .

Is it a typo or intentional that *iota* is spelled out and not  $\iota$  in the figure caption?

prop:nonabneeded

**Proposition 4.18.** *The map  $\iota$  descends to a cononical isomorphism  $\tilde{\mathcal{T}}_{\nabla}^{/1} \cong \tilde{\mathcal{T}}^{/1}$ .*

*Proof.* The Conway relation applies only in  $s$ -filtered degree one and above, and hence has no effect on  $\tilde{\mathcal{T}}^{/1}$ .  $\square$

In light of this, we write only  $\tilde{\mathcal{T}}^{/1}$ , rather than  $\tilde{\mathcal{T}}_{\nabla}^{/1}$ . Now let  $\tilde{\mathcal{T}}^{1/2}$  denote  $\tilde{\mathcal{T}}^1/\tilde{\mathcal{T}}^2$ , and  $\tilde{\mathcal{T}}_{\nabla}^{1/2}$  denote  $\tilde{\mathcal{T}}_{\nabla}^1/\tilde{\mathcal{T}}_{\nabla}^2$ .

Finally, we establish a key technical result about low  $s$ -degree quotients of the Conway quotient:

prop:divbybexists

**Proposition 4.19.** *The  $\mathbb{C}$ -linear map given by post-composing  $\iota$  with multiplication by  $b$ ,*

$$m_b : \tilde{\mathcal{T}}^{1/1} \rightarrow \tilde{\mathcal{T}}_{\nabla}^{1/2}$$

*is injective, and its image is  $\tilde{\mathcal{T}}_{\nabla}^{1/2}$ .*

*Proof.* We first prove that the image of  $m_b$  is  $\tilde{\mathcal{T}}_{\nabla}^{1/2}$ . The quotient  $\tilde{\mathcal{T}}^{1/1}$  is spanned by cosets of tangles  $T$ . It is immediate that the image of  $m_b$  is contained in  $\tilde{\mathcal{T}}^{1/2}$ , as  $m_b(T) = bT$  represents an element in  $\tilde{\mathcal{T}}^1$ .

Conversely, any element  $y \in \tilde{\mathcal{T}}^{1/2}$  is (non-uniquely) represented as a sum of the form  $\sum_{i=1}^k T_i + b \sum_{j=1}^l T'_j$ , where  $T_i$  are tangles with one double point each, and  $T'_j$  are arbitrary tangles. Then, by the Conway relation, each  $T_i = b \cdot T_i^C$ , where  $T_i^C$  denotes the tangle where the double point in  $T_i$  has been smoothed. Thus,  $y = b \left( \sum_{i=1}^k T_i^C + \sum_{j=1}^l T'_j \right)$ , and therefore  $y$  is in the image of  $m_b$ , and  $m_b$  is surjective onto  $\tilde{\mathcal{T}}_{\nabla}^{1/2}$ .

To prove the injectivity of  $m_b$ , we construct a one-sided inverse: a “division by  $b$ ” map  $q_b$  on  $\tilde{\mathcal{T}}_{\nabla}^{1/2}$ , as follows.

For a tangle diagram  $D_T$  (representing a tangle  $T$ ) and a crossing  $x$  of  $D_T$ , let  $\epsilon(x) \in \{\pm 1\}$  be the sign of  $x$ , and  $D_T|_{x \rightarrow \smile}$  be the diagram  $D_T$  with  $x$  replaced by a smoothing. We first define a map  $q_b$  from the free  $\mathbb{C}[b]$ -module spanned by tangle diagrams, to  $\tilde{\mathcal{T}}^{1/1}$ , as the linear extension of the following:

$$\begin{aligned} b^k D_T &\xrightarrow{q_b} 0 \text{ if } k \geq 2, \\ b D_T &\xrightarrow{q_b} D_T, \\ D_T &\xrightarrow{q_b} \frac{1}{2} \sum_{x \text{ crossing of } T} \epsilon(x) D_T|_{x \rightarrow \smile}. \end{aligned}$$

We claim that this descends to a well defined map  $q_b : \tilde{\mathcal{T}}_{\nabla}^{1/2} \rightarrow \tilde{\mathcal{T}}^{1/1}$ . It is straightforward to check that the Reidemeister moves are in the kernel of  $q_b$ . We also need to verify that  $\tilde{\mathcal{T}}_{\nabla}^2$  and the Conway relation are in the kernel.

An element of  $\tilde{\mathcal{T}}_{\nabla}^2$  can be represented as a sum of terms  $b^k D_T \in \tilde{\mathcal{T}}_{\nabla}^2$ , where  $D_T$  is a tangle diagram with or without double points. If  $k \geq 2$  then  $q_b(b^k D_T) = 0$ . If  $k = 1$ , then  $D_T$  has a double point, so  $q_b(b D_T) = D_T$  is zero in  $\tilde{\mathcal{T}}^{1/1}$ . If  $k = 0$ , then  $D_T$  has at least two double points. Smoothing a crossing interferes with at most one of the double points, so  $q_b(D_T)$  can be written as a sum of terms with at least one double point each. Hence  $q_b(D_T) \in \tilde{\mathcal{T}}^1$  as well.

To show that the Conway relation vanishes, note that  $q_b(\bowtie) = q_b(\bowtie^* - \bowtie^*)$  is a sum with two types of terms: those which smooth a crossing that is a part of the double point, and those which smooth a crossing that is not. In the latter case, the double points are unchanged, so these terms are in  $\tilde{\mathcal{T}}_{\nabla}^1$ . From the terms

where the crossings forming the double point are smoothed, we get

$$q_b \left( \begin{array}{c} \diagup \diagdown \\ \diagdown \diagup \end{array} - \begin{array}{c} \diagdown \diagup \\ \diagup \diagdown \end{array} \right) = \frac{1}{2} \updownarrow - (-1) \frac{1}{2} \updownarrow = \updownarrow = q_b \left( \begin{array}{c} \diagup \diagdown \\ \diagup \diagdown \end{array} \right),$$

as the Conway relation requires. Thus,  $q_b$  is well-defined on  $\tilde{\mathcal{T}}_{\nabla}^{1/2}$ .

Finally,  $q_b$  is clearly a one-sided inverse for  $m_b$ , and therefore,  $m_b$  is injective.  $\square$

cor:divbyb

**Corollary 4.20.** *The map  $m_b : \tilde{\mathcal{T}}^{1/1} \rightarrow \tilde{\mathcal{T}}_{\nabla}^{1/2}$  is a  $\mathbb{C}$ -linear isomorphism with inverse  $q_b : \tilde{\mathcal{T}}_{\nabla}^{1/2} \rightarrow \tilde{\mathcal{T}}^{1/1}$ .*

Notice that both  $m_b$  and  $q_b$  shift the filtered degrees. The Goldman-bracket and Turaev cobracket are also degree-shifting, and these shifts will be realised by  $m_b$  and  $q_b$ . The following fact in particular will be important in the construction of the Goldman bracket:

lem:mbOnCircle

**Lemma 4.21.** *The map  $m_b$  restricts to an injective  $\mathbb{C}$ -linear map*

$$m_b : \tilde{\mathcal{T}}^{1/1}(\bigcirc) \rightarrow \tilde{\mathcal{T}}_{\nabla}^{1/2}(\bigcirc\bigcirc).$$

*Proof.* Elements of  $\tilde{\mathcal{T}}^{1/1}$  are linearly generated by the cosets of knots. Given a knot  $K$ ,  $bK$  is equal in  $\tilde{\mathcal{T}}^{1/2}$  to a difference of two two-component links, by a single use of the Conway relation. Hence, the codomain is  $\tilde{\mathcal{T}}^{1/2}(\bigcirc\bigcirc)$ . Injectivity is inherited from  $m_b$  on  $\tilde{\mathcal{T}}^{1/1}$ .  $\square$

Note that this restriction of  $m_b$  is not surjective to  $\tilde{\mathcal{T}}^{1/2}(\bigcirc\bigcirc)$ , for example, two-component links with a double point involving only one component are not in the image.

We introduce the same notation on the associated graded side:

**Definition 4.22.** For a skeleton  $S$ , let  $\tilde{\mathcal{A}}_{\nabla}(S)$  denote the image  $\text{gr } \iota(\tilde{\mathcal{A}}(S))$ .

By a straightforward calculation of the degree shifting associated graded maps we obtain:

rem:grdivbyb

**Proposition 4.23.** *The associated graded map of  $m_b$  is an isomorphism  $\text{gr } m_b = m_a : \tilde{\mathcal{A}}^{1/1} \rightarrow \tilde{\mathcal{A}}^{1/2}$ , which multiplies chord diagrams by  $a$ . The inverse is the isomorphism  $\text{gr } q_b = q_a : \tilde{\mathcal{A}}^{1/2} \rightarrow \tilde{\mathcal{A}}^{1/1}$ . The isomorphism  $q_a$  divides by ‘ $a$ ’ if a factor of ‘ $a$ ’ is available; otherwise uses the Conway relation to smooth an  $s$ - $s$  chord and obtain a factor of ‘ $a$ ’ first. Furthermore,  $m_a$  restricts to an injective map  $m_a : \tilde{\mathcal{A}}^{1/1}(\bigcirc) \rightarrow \tilde{\mathcal{A}}^{1/2}(\bigcirc\bigcirc)$ .  $\square$*

check what happens with framed R1 when we mod out by the first step of the s-filtration...

sec:notation

**4.7. Notation conventions.** In this Section we have introduced extensive notation, and we are about to use all of it to prove our main results in Section 5. For convenience, we include a summary here:

- $\mathbb{C}\tilde{\mathcal{T}}$  is the space of  $\mathbb{C}$ -linear combinations of framed tangles in  $M_p$
- $\mathbb{C}\tilde{\mathcal{T}}(S)$  is the space of  $\mathbb{C}$ -linear combinations of framed tangles in  $M_p$  with skeleton  $S$ .

- $\mathbb{C}\tilde{\mathcal{T}}(\bigcirc)$  is the space of  $\mathbb{C}$ -linear combinations of framed knots in  $M_p$ .
- $\tilde{\mathcal{T}}_t$  is the  $t$ 'th filtered component of  $\mathbb{C}\tilde{\mathcal{T}}$  in the total (or  $t$ -) filtration: the  $\mathbb{C}$ -linear span of framed tangles with at least  $t$  double points or framing changes.
- $\tilde{\mathcal{T}}^s$  is the  $s$ 'th filtered component of  $\mathbb{C}\tilde{\mathcal{T}}$  in the strand (or  $s$ -) filtration: the  $\mathbb{C}$ -linear span of framed tangles in  $M_p$  with at least  $s$  strand-strand double points or framing changes.
- $\tilde{\mathcal{T}}_t^s = \tilde{\mathcal{T}}_t \cap \tilde{\mathcal{T}}^s$ .
- $\tilde{\mathcal{T}}^{/s} = \mathbb{C}\tilde{\mathcal{T}} / \tilde{\mathcal{T}}^s$ .
- $\tilde{\mathcal{T}}^{1/2} := \tilde{\mathcal{T}}^1 / \tilde{\mathcal{T}}^2$ .
- $\tilde{\mathcal{A}}$  is the associated graded space of  $\mathbb{C}\tilde{\mathcal{T}}$  under the  $t$ -filtration, spanned admissible chord diagrams modulo admissible  $4T$  relations.
- $\tilde{\mathcal{A}}_t := \tilde{\mathcal{T}}_t / \tilde{\mathcal{T}}_{t+1}$  is the degree  $t$  component of  $\tilde{\mathcal{A}}$  which consists of all admissible chord diagrams in  $\tilde{\mathcal{A}}$  with exactly  $t$  chords.
- $\tilde{\mathcal{A}}^{\geq s} := \prod_t \tilde{\mathcal{T}}_t^s / \tilde{\mathcal{T}}_{t+1}^s$  is the  $s$ 'th filtered component of  $\tilde{\mathcal{A}}$  in the induced  $s$ -filtration, spanned by chord diagrams with  $t$  chords, of which at least  $s$  are strand-strand.
- $\tilde{\mathcal{A}}^{/s} := \tilde{\mathcal{A}} / \tilde{\mathcal{A}}^{\geq s}$ .
- $\mathbb{C}\tilde{\mathcal{T}}_{\nabla}$  is the quotient of  $\mathbb{C}\tilde{\mathcal{T}}[[a]]$  by the Conway relation.
- $\tilde{\mathcal{T}}_{\nabla,t}$  is the  $t$ -th total filtered component of  $\mathbb{C}\tilde{\mathcal{T}}_{\nabla}$ , where  $a$  is of  $t$ -degree one. Similarly,  $\tilde{\mathcal{T}}_{\nabla}^s$  is the  $s$ -th filtered component in the strand filtration, where  $a$  is of  $s$ -degree one. The notation for degree quotients is as before.
- $\tilde{\mathcal{A}}_{\nabla}$  is the quotient of  $\tilde{\mathcal{A}}[[a]]$  by the chord diagram Conway relation.  $\tilde{\mathcal{A}}_{\nabla,t}$  denotes the degree  $t$  component,  $\tilde{\mathcal{A}}_{\nabla}^s$  the  $s$ -th filtered component, and  $\tilde{\mathcal{A}}_{\nabla,t}^s = \tilde{\mathcal{A}}_{\nabla,t} \cap \tilde{\mathcal{A}}_{\nabla}^s$ .
- $\mathbb{C}\tilde{\mathcal{T}}_{\nabla}(S)$  is the image of  $\mathbb{C}\tilde{\mathcal{T}}_{\nabla}(S)$  under the natural map  $\iota : \mathbb{C}\tilde{\mathcal{T}} \rightarrow \mathbb{C}\tilde{\mathcal{T}}_{\nabla}$ .

## 5. IDENTIFYING THE GOLDMAN-TURAEV LIE BIALGEBRA

In this section we establish our main results: we identify the Goldman-Turaev Lie bialgebra in the low  $s$ -filtered degree quotients of  $\mathbb{C}\tilde{\mathcal{T}}$ , and show that the Kontsevich integral induces a homomorphic expansion. The arguments follow the outline summarized in Section 2, and obtain the Goldman bracket and the self-intersection map  $\mu$  as induced operations. In turn, the homomorphicity of the Kontsevich integral follows from the naturality of the construction.

**5.1. The Goldman Bracket.** Recall from Section 3.2 that  $D_p$  denotes the  $p$ -punctured disc,  $\pi$  is its fundamental group, and  $|\mathbb{C}\pi|$  is the linear quotient  $|\mathbb{C}\pi| := \mathbb{C}\pi / [\mathbb{C}\pi, \mathbb{C}\pi]$ , which is linearly generated by homotopy classes of free loops in  $D_p$ . The Goldman bracket (Definition 3.2) is a lie bracket  $[\cdot, \cdot]_G : |\mathbb{C}\pi| \otimes |\mathbb{C}\pi| \rightarrow |\mathbb{C}\pi|$ . We start by identifying  $|\mathbb{C}\pi|$  in a low degree quotient of  $\mathbb{C}\tilde{\mathcal{T}}(\bigcirc)$  through a map  $\beta$  induced by the bottom projection.

IdentifyingGTinCON

IdentifybracketinCON

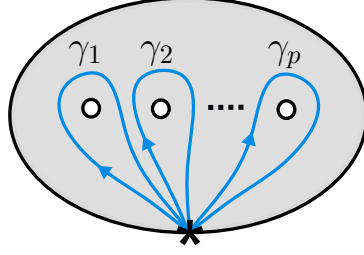
FIGURE 19. The standard generating curves of  $\pi$ .

fig:GenCurves

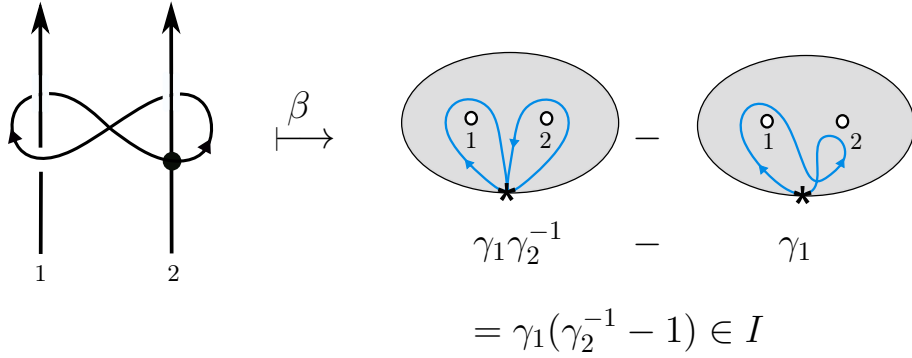
FIGURE 20. Example calculation demonstrating that  $\beta$  is a filtered map.

fig:BetaFiltered

prop:BotProj

**Proposition 5.1.** *The bottom projection  $M_p \rightarrow D_p \times \{0\}$  induces a surjective filtered map*

$$\beta : \mathbb{C}\tilde{\mathcal{T}}(\mathbb{O}) \rightarrow |\mathbb{C}\pi|.$$

*Proof.* By the framed Reidemeister Theorem, framed knots in  $\mathbb{C}\tilde{\mathcal{T}}(\mathbb{O})$  are faithfully represented by knot diagrams in  $D_p \times \{0\}$  – regular projections to the bottom with over/under information – modulo the framed Reidemeister moves (weak R1, R2, and R3). Diagrammatically, the bottom projection forgets the over/under information, in other words, imposes the relation  $\nearrow = \nwarrow$ . The images of the Reidemeister moves follow from the corresponding moves generating homotopies of immersed free loops, hence  $\beta$  is well-defined. The projection is clearly surjective as any loop can be lifted to a framed knot by introducing arbitrary under/over information at the crossings and imposing the blackboard framing.

The statement that  $\beta$  is filtered means that step  $k$  of the the Vassiliev  $t$ -filtration in  $\mathbb{C}\tilde{\mathcal{T}}(\mathbb{O})$  projects to step  $k$  of the filtration on  $|\mathbb{C}\pi|$  induced by the  $\mathbb{I}$ -adic filtration of  $\pi$ . Note that strand-strand double points and framing changes are in the kernel of  $\beta$ , thus, we only have something to prove for knots with  $k$  strand-pole double points.

Let  $\gamma_1, \dots, \gamma_p$  denote the standard generators of  $\pi$  as in Figure 19. A knot  $K \in \mathbb{C}\tilde{\mathcal{T}}(\mathbb{O})$  maps to a free loop in  $|\mathbb{C}\pi|$ , whose conjugacy class in  $\pi$  is represented as a word in the generators  $\gamma_i$ . A pole-strand double point on pole  $j$  maps to a difference between two curves passing on either side of the  $j$ 'th puncture (as in Figure 20). Therefore, one of the words in  $\mathbb{C}\pi$  representing these curves can be obtained from the other by inserting a single letter  $\gamma_j^{\pm 1}$ . The double point, which represents the difference, thus maps to a product with a factor of  $(\gamma_j^{\pm 1} - 1)$ , and a knot with  $k$  pole-strand double points maps to a product with  $k$  factors of the form  $(\gamma_j^{\pm 1} - 1)$ . This is by definition an element in  $\mathcal{I}^k$ .  $\square$

prop:kerbeta

**Proposition 5.2.** *The kernel of  $\beta$  is  $\tilde{\mathcal{T}}^1(\mathbb{O})$ , and thus,  $\beta$  descends to a filtered linear isomorphism  $\beta : \tilde{\mathcal{T}}^1(\mathbb{O}) \rightarrow |\mathbb{C}\pi|$ .*

*Proof.* Two framed knots in  $\mathbb{C}\tilde{\mathcal{T}}(\mathbb{O})$  project to the same loop in  $|\mathbb{C}\pi|$  if and only if they differ by framing changes and (strand-strand) crossing changes, which generate exactly the step 1 of the  $s$ -filtration, that is,  $\tilde{\mathcal{T}}^1(\mathbb{O})$ .  $\square$

Recall that  $\tilde{\mathcal{A}}$  denotes the (degree completed) associated graded space of  $\mathbb{C}\tilde{\mathcal{T}}$  with respect to the  $t$ -filtration, described as the space of admissible chord diagrams on a circle skeleton, as in Definition 4.6. The  $s$ -filtration on  $\mathbb{C}\tilde{\mathcal{T}}$  induces a corresponding  $s$ -filtration on  $\tilde{\mathcal{A}}$ , and  $\tilde{\mathcal{A}}^{\geq i}(\mathbb{O})$  denotes the  $i$ -th  $s$ -filtered component of  $\tilde{\mathcal{A}}(\mathbb{O})$ . We also denote  $\tilde{\mathcal{A}}^i(\mathbb{O}) = \tilde{\mathcal{A}}(\mathbb{O}) / \tilde{\mathcal{A}}^{\geq i}(\mathbb{O})$ .

Recall from Section 3.2 that the associated graded vector space of  $|\mathbb{C}\pi|$  is  $|\mathbb{F}\mathbb{A}|$ , where  $\mathbb{F}\mathbb{A} = \mathbb{F}\mathbb{A}\langle x_1, \dots, x_p \rangle$  denotes the free associative algebra over  $\mathbb{C}$ , and the linear quotient  $|\mathbb{F}\mathbb{A}| = \mathbb{F}\mathbb{A} / [\mathbb{F}\mathbb{A}, \mathbb{F}\mathbb{A}]$  is the graded  $\mathbb{C}$ -vector space generated by cyclic words in the letters  $x_1, \dots, x_p$ . The graded Goldman bracket is a map  $[-, -]_{\text{gr}} : |\mathbb{F}\mathbb{A}| \otimes |\mathbb{F}\mathbb{A}| \rightarrow |\mathbb{F}\mathbb{A}|$ , as defined in Proposition 3.6. Denote the degree completions of  $\mathbb{F}\mathbb{A}$  and  $|\mathbb{F}\mathbb{A}|$  by  $\widehat{\mathbb{F}\mathbb{A}}$  and  $|\widehat{\mathbb{F}\mathbb{A}}|$ . By applying the associated graded functor to  $\beta$ , we identify  $|\widehat{\mathbb{F}\mathbb{A}}|$  as follows:

prop:gr\_beta

**Proposition 5.3.** *The associated graded map  $\text{gr } \beta : \tilde{\mathcal{A}}(\mathbb{O}) \rightarrow |\widehat{\mathbb{F}\mathbb{A}}|$  has kernel  $\tilde{\mathcal{A}}^{\geq 1}(\mathbb{O})$ . Hence,  $\text{gr } \beta$  descends to an isomorphism  $\text{gr } \beta : \tilde{\mathcal{A}}^1(\mathbb{O}) \rightarrow |\widehat{\mathbb{F}\mathbb{A}}|$ .*

*Proof.* The statement follows from applying the associated graded functor to the filtered short exact sequence

$$0 \longrightarrow \tilde{\mathcal{T}}^1(\mathbb{O}) \longrightarrow \tilde{\mathcal{T}}(\mathbb{O}) \xrightarrow{\beta} |\mathbb{C}\pi| \longrightarrow 0.$$

The filtrations on  $\tilde{\mathcal{T}}^1(\mathbb{O})$  and  $|\mathbb{C}\pi|$  are induced from the filtration on  $\tilde{\mathcal{T}}(\mathbb{O})$ , as in Lemma 2.3, therefore the associated graded sequence is also exact.  $\square$

rem:ChorsOnPoles

*Remark 5.4.* In  $\tilde{\mathcal{A}}^1(\mathbb{O})$  chord diagrams with any strand-strand chords are zero. Thus,  $\tilde{\mathcal{A}}^1(\mathbb{O})$  is spanned by chord diagrams on poles and a single circle strand, with strand-pole chords only: for an example see the left of Figure 21. Note also that all admissible 4T relations involve a strand-strand chord, and are zero in

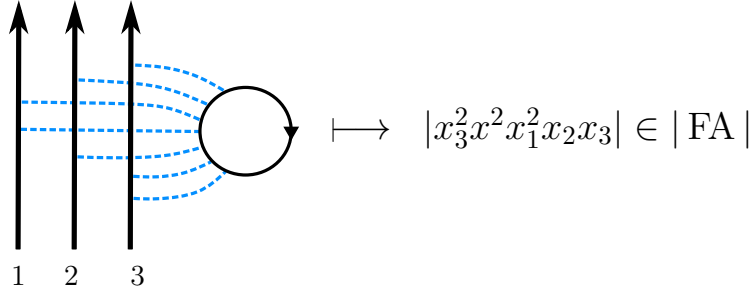


FIGURE 21. An example demonstrating how chord diagrams with no strand-strand chords can be read as cyclic words in  $|FA|$ .

fig:CycWord

$\tilde{\mathcal{A}}^{/1}$ . This means that chord endings on the poles commute, and there are no further relations. Such a chord diagram corresponds naturally to a cyclic word by labeling the poles with  $x_1, \dots, x_p$  and reading along the circle skeleton, as on the right of Figure 21. Indeed, this is an isomorphism, and gives the explicit description of  $\text{gr } \beta$ .

Having identified the domain of the Goldman Bracket,  $|\mathbb{C}\pi| \otimes |\mathbb{C}\pi|$ , as  $\tilde{\mathcal{T}}^{/1}(\mathbb{O}) \otimes \tilde{\mathcal{T}}^{/1}(\mathbb{O})$  through the identification  $\beta$ , we can now show that the Goldman bracket is induced – in the sense of Section 2 – by the stacking commutator on  $\mathbb{C}\tilde{\mathcal{T}}$ .

thm:bracketsnake

**Theorem 5.5.** *Let  $\lambda_1 : \tilde{\mathcal{T}}_{\nabla}^{/2}(\mathbb{O}) \otimes \tilde{\mathcal{T}}_{\nabla}^{/2}(\mathbb{O}) \rightarrow \tilde{\mathcal{T}}_{\nabla}^{/2}(\mathbb{O})$  denote the stacking product. Let  $\lambda_2$  denote the opposite product given by  $\lambda_2(K_1, K_2) = K_2 K_1$ . The stacking commutator  $\lambda = \lambda_1 - \lambda_2$  induces a unique map  $\hat{\eta} : \tilde{\mathcal{T}}^{/1}(\mathbb{O}) \otimes \tilde{\mathcal{T}}^{/1}(\mathbb{O}) \rightarrow \tilde{\mathcal{T}}^{/1}(\mathbb{O})$ , in the sense of the commutative diagram in Figure 22. The map  $\hat{\eta}$  coincides with the Goldman bracket on  $|\mathbb{C}\pi|$  via the identification  $\beta : \tilde{\mathcal{T}}^{/1}(\mathbb{O}) \xrightarrow{\cong} |\mathbb{C}\pi|$ , that is,*

$$[-, -]_G = \beta \circ \hat{\eta} \circ (\beta^{-1} \otimes \beta^{-1}).$$

*Proof.* The vector space  $\tilde{\mathcal{T}}_{\nabla}^{/2}(\mathbb{O})$  is generated by the equivalence classes of knots in  $M_p$ . For  $K_1, K_2 \in \tilde{\mathcal{T}}$ , we abuse notation and denote by  $K_1 \otimes K_2$  the class of  $K_1 \otimes K_2$  in  $\tilde{\mathcal{T}}_{\nabla}^{/2}(\mathbb{O}) \otimes \tilde{\mathcal{T}}_{\nabla}^{/2}(\mathbb{O})$ . The stacking commutator  $\lambda(K_1 \otimes K_2) = K_1 K_2 - K_2 K_1$  is the difference between placing  $K_2$  above or below  $K_1$  in  $D_p \times I$ .

We first show that the right hand square of Figure 22 commutes. Regularly project  $K_1, K_2$  and their stacking products to the bottom  $D_p$  to obtain knot diagrams  $D_1$  and  $D_2$ , and link diagrams  $D_1 D_2$  and  $D_2 D_1$ . A *mixed crossing* of a link diagram be a crossing where the two strands belong to separate components. Notice that  $D_2 D_1$  is precisely  $D_1 D_2$  with all mixed crossings flipped.

Number the mixed crossings of  $D_1 D_2$  from 1 to  $r$ , and let  $L_i$  denote the link diagram where the first  $i$  mixed crossings have been flipped. Specifically,  $L_0 = D_1 D_2$  and  $L_r = D_2 D_1$ . Then  $L_0 - L_r = D_1 D_2 - D_2 D_1$  can be written as a



$$\begin{array}{ccccccc}
0 & \longrightarrow & \text{Ker} & \longrightarrow & \tilde{\mathcal{T}}_{\nabla}^{1/2}(\bigcirc) \otimes \tilde{\mathcal{T}}_{\nabla}^{1/2}(\bigcirc) & \longrightarrow & \tilde{\mathcal{T}}^{1/1}(\bigcirc) \otimes \tilde{\mathcal{T}}^{1/1}(\bigcirc) \longrightarrow 0 \\
& & \downarrow 0 & & \downarrow \lambda & & \downarrow 0 \\
0 & \longrightarrow & \tilde{\mathcal{T}}_{\nabla}^{1/2}(\bigcirc\bigcirc) & \longrightarrow & \tilde{\mathcal{T}}_{\nabla}^{1/2}(\bigcirc\bigcirc) & \longrightarrow & \tilde{\mathcal{T}}^{1/1}(\bigcirc\bigcirc) \longrightarrow 0 \\
& & \uparrow m_b & & \nwarrow \hat{\eta} & & \\
& & \tilde{\mathcal{T}}^{1/1}(\bigcirc) & & & & 
\end{array}$$

$\eta$  (dashed arrow from Ker to  $\tilde{\mathcal{T}}^{1/1}(\bigcirc) \otimes \tilde{\mathcal{T}}^{1/1}(\bigcirc)$ )  
 $\hat{\eta}$  (dashed arrow from  $\tilde{\mathcal{T}}^{1/1}(\bigcirc)$  to  $\tilde{\mathcal{T}}_{\nabla}^{1/2}(\bigcirc\bigcirc)$ )

FIGURE 22. Recovering the Goldman bracket. The horizontal maps are the natural quotient and inclusion maps, and Ker denotes the kernel of the consecutive projection. The map  $m_b$  denotes multiplication by  $b$  (Lemma 4.21).

fig:Snakeforbracket

telescopic sum:

eq:Telescope

$$(5.1) \quad D_1 D_2 - D_2 D_1 = (L_0 - L_1) + (L_1 - L_2) + \dots + (L_{r-1} - L_r).$$

In the sum, each term in parenthesis is a two-component link with a single mixed double point, with a sign (the crossing sign of the  $i$ -th mixed crossing). Thus,  $\lambda(K_1, K_2) \in \tilde{\mathcal{T}}_{\nabla}^1$ , and maps to zero in  $\tilde{\mathcal{T}}_{\nabla}^{1/1}$ . Hence, the right hand square commutes.

We now turn to the left square of the diagram. The kernel of the projection map

$$\tilde{\mathcal{T}}_{\nabla}^{1/2}(\bigcirc) \otimes \tilde{\mathcal{T}}_{\nabla}^{1/2}(\bigcirc) \rightarrow \tilde{\mathcal{T}}_{\nabla}^{1/1}(\bigcirc) \otimes \tilde{\mathcal{T}}_{\nabla}^{1/1}(\bigcirc)$$

is generated by  $\tilde{\mathcal{T}}_{\nabla}^{1/2}(\bigcirc) \otimes \tilde{\mathcal{T}}_{\nabla}^{1/2}(\bigcirc)$  and  $\tilde{\mathcal{T}}_{\nabla}^{1/2}(\bigcirc) \otimes \tilde{\mathcal{T}}_{\nabla}^{1/2}(\bigcirc)$ . Suppose that  $K_1 \otimes K_2$  is in  $\tilde{\mathcal{T}}_{\nabla}^{1/2}(\bigcirc) \otimes \tilde{\mathcal{T}}_{\nabla}^{1/2}(\bigcirc)$ ; without loss of generality assume that  $K_1$  is a knot with one double point. Then, by Equation 5.1,  $\lambda(K_1 \otimes K_2)$  can be written as a telescopic sum of links with two double points each, hence it is zero in  $\tilde{\mathcal{T}}_{\nabla}^{1/2}(\bigcirc\bigcirc)$ . Therefore, the left square commutes.

As in Section 2, then  $\lambda$  induces a unique map

$$\eta : \tilde{\mathcal{T}}^{1/1}(\bigcirc) \otimes \tilde{\mathcal{T}}^{1/1}(\bigcirc) \rightarrow \tilde{\mathcal{T}}_{\nabla}^{1/2}(\bigcirc\bigcirc).$$

We can now identify  $\eta$  as the Goldman bracket. The isomorphism  $\beta$  gives  $\tilde{\mathcal{T}}^{1/1}(\bigcirc) \cong |\mathbb{C}\pi|$  (Proposition 5.2) identifies the domain of  $\eta$  with the domain of the Goldman bracket. We will argue that the image of  $\eta$  also lies in  $\tilde{\mathcal{T}}^{1/1}(\bigcirc) \cong |\mathbb{C}\pi|$ .

By Equation (5.1),  $\lambda(K_1, K_2)$  can be written a sum of  $r$  terms, each with one mixed double point. Applying the Conway relation to each of the  $r$  terms of the telescopic sum by smoothing the mixed double points changes the skeletons from

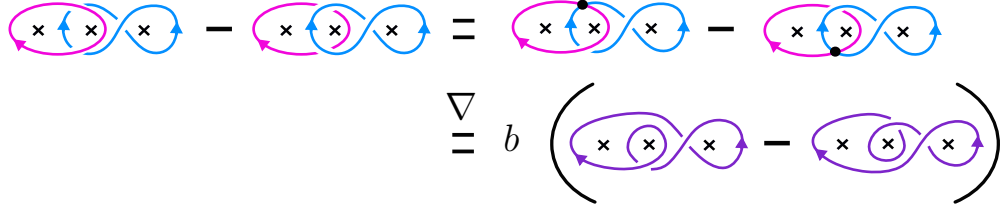


FIGURE 23. Example commutator bracket computation. The first equality is true after canceling terms in a telescoping expansion of the double points.

fig:combracket

two circles to one circle, and introduces a factor of  $b$ :

$$(5.2) \quad \lambda(K_1 \otimes K_2) = D_1 D_2 - D_2 D_1 \stackrel{\nabla}{=} b(\epsilon_1 K_{s_1} + \epsilon_2 K_{s_2} + \dots + \epsilon_r K_{s_r}).$$

Here  $K_{s_i}$  denotes the knot obtained from  $L_{i-1} - L_i$  by smoothing the mixed double point (which is obtained from the  $i$ -th mixed crossing), and  $\epsilon_i$  is the sign of the  $i$ -th mixed crossing. That is,  $\lambda(K_1, K_2) \in b\tilde{\mathcal{T}}_{\nabla}^{1/2}(\mathcal{O})$ . In other words,  $\eta$  factors through  $\tilde{\mathcal{T}}^1(\mathcal{O})$ , which embeds in  $\tilde{\mathcal{T}}_{\nabla}^{1/2}(\mathcal{O}, \mathcal{O})$  via the multiplication by  $b$  map  $m_b$ , by Lemma 4.21. Hence, we obtain the map  $\hat{\eta} : \tilde{\mathcal{T}}^1(\mathcal{O}) \otimes \tilde{\mathcal{T}}^1(\mathcal{O}) \rightarrow \tilde{\mathcal{T}}^1(\mathcal{O})$ , as needed.

Finally, we check that  $\hat{\eta}$  coincides with the Goldman bracket via the identification  $\beta$ . For curves  $\gamma_1 \otimes \gamma_2 \in \tilde{\mathcal{T}}^1(\mathcal{O}) \otimes \tilde{\mathcal{T}}^1(\mathcal{O})$ , let  $K_1 \otimes K_2 \in \tilde{\mathcal{T}}_{\nabla}^{1/2}(\mathcal{O}) \otimes \tilde{\mathcal{T}}_{\nabla}^{1/2}(\mathcal{O})$  be an arbitrary pre-image (vertical lift) of  $\gamma_1 \otimes \gamma_2$ . Then

$$\eta(\gamma_1 \otimes \gamma_2) = \frac{\lambda(K_1 \otimes K_2)}{b} \in \tilde{\mathcal{T}}^1(\mathcal{O}),$$

where we use the notation  $\frac{1}{b}$  to mean composition with  $q_b$ . The Goldman bracket (Definition 3.2) is precisely a sum of smoothings of the mixed crossings of  $\gamma_1$  and  $\gamma_2$ . The only thing to check is that the crossing signs coincide with the negative signs of the local coordinate systems in the Goldman bracket definition, which is indeed the case. See Figure 23 for an example.  $\square$

Recall that the graded Goldman bracket (Proposition 3.6) is a linear map  $[-, -]_{\text{gr } G} : |\text{FA}| \otimes |\text{FA}| \rightarrow |\text{FA}|$ , and by Proposition 5.3 we have an identification  $\text{gr } \beta : |\text{FA}| \xrightarrow{\cong} \tilde{\mathcal{A}}^1(\mathcal{O})$ . Applying the associated graded functor – with respect to the total filtration – to the diagram in Figure 22, we obtain the commutative diagram in Figure 24 and recover the graded Goldman bracket:

**Corollary 5.6.** *The diagram in Figure 24 commutes, the rows are exact,  $\text{gr } \eta$  is the induced connecting homomorphism, and  $\text{gr } \hat{\eta}$  agrees with the associated graded Goldman bracket via the identification  $\text{gr } \beta : \tilde{\mathcal{A}}^1(\mathcal{O}) \xrightarrow{\cong} |\text{FA}|$ . In other words,*

$$\text{gr}[\cdot, \cdot]_G = \text{gr } \beta \circ \text{gr } \hat{\eta} \circ (\text{gr } \beta^{-1} \otimes \text{gr } \beta^{-1}).$$

snakefor\_gr\_bracket

$$\begin{array}{ccccccc}
0 & \longrightarrow & \text{Ker} & \longrightarrow & \tilde{\mathcal{A}}_{\nabla}^{1/2}(\bigcirc) \otimes \tilde{\mathcal{A}}_{\nabla}^{1/2}(\bigcirc) & \longrightarrow & \tilde{\mathcal{A}}^{1/1}(\bigcirc) \otimes \tilde{\mathcal{A}}^{1/1}(\bigcirc) \longrightarrow 0 \\
& & \downarrow 0 & & \downarrow \text{gr } \lambda & & \downarrow 0 \\
0 & \longrightarrow & \tilde{\mathcal{A}}_{\nabla}^{1/2}(\bigcirc\bigcirc) & \longrightarrow & \tilde{\mathcal{A}}_{\nabla}^{1/2}(\bigcirc\bigcirc) & \longrightarrow & \tilde{\mathcal{A}}_{\nabla}^{1/1}(\bigcirc\bigcirc) \longrightarrow 0 \\
& & \uparrow & & \uparrow \text{gr } \hat{\eta} & & \\
& & \tilde{\mathcal{A}}^{1/1}(\bigcirc) & \xleftarrow{\text{gr } \eta} & & & 
\end{array}$$

FIGURE 24. Recovering the graded Goldman bracket by applying the associated graded functor to the commutative diagram of Figure 22.

Snakefor\_gr\_bracket

*Proof.* All arrows in the diagram in Figure 22 are filtered maps with respect to the total filtration; the rows are exact; and the total filtrations on the left and right hand sides are induced from the total filtration in the middle. Hence, Corollary 2.4 applies, and hence the  $\text{gr}$  functor gives a commutative diagram with exact rows, as in Figure 24. By the uniqueness of the connecting homomorphism, we know that it is  $\text{gr } \eta$ . By the functoriality of the associated graded, the graded Goldman bracket is given by

$$\text{gr}[\cdot, \cdot]_G = \text{gr } \beta \circ \text{gr } \hat{\eta} \circ (\text{gr } \beta^{-1} \otimes \text{gr } \beta^{-1}).$$

□

ex:grGoldman

**Example 5.7.** While the Corollary 5.6 follows from abstract considerations, let us demonstrate the on an example the explicit calculation of the graded bracket. Recall from Remark 5.4 that in  $\tilde{\mathcal{A}}^{1/1}$  chord endings on the poles commute. The identification  $\text{gr } \beta$  works by assigning a letter  $x_1, \dots, x_p$  to each pole, and reading off the cyclic word given by the chords along the circle skeleton component, as in Figure 21.

We compute the graded bracket of the words  $|x_1 x_2^2|$  and  $|x_2 x_3^2|$ , via  $\text{gr } \beta$ . The two cyclic words correspond to chord diagrams in  $\tilde{\mathcal{A}}^{1/1}(\bigcirc)$ , which we then consider in (lift to)  $\tilde{\mathcal{A}}_{\nabla}^{1/2}(\bigcirc)$ . The map  $\text{gr } \lambda$  is the stacking commutator of these diagrams, as shown in Figure 25. This lies in  $\tilde{\mathcal{A}}_{\nabla}^{1/2}(\bigcirc\bigcirc)$ , which is easiest to see via applying a 4T relation for the letter coincidence  $x_2$ , as shown in Figure 25. In turn, via an application of the Conway relation, it is easy to see that the element of  $\tilde{\mathcal{A}}^{1/1}(\bigcirc)$  which maps to this via multiplication by  $b$  is  $|x_1^2 x_2 x_3^2| - |x_1^2 x_3^2 x_2|$ . This is precisely the value of the graded Goldman bracket: compare also with Figure 6.

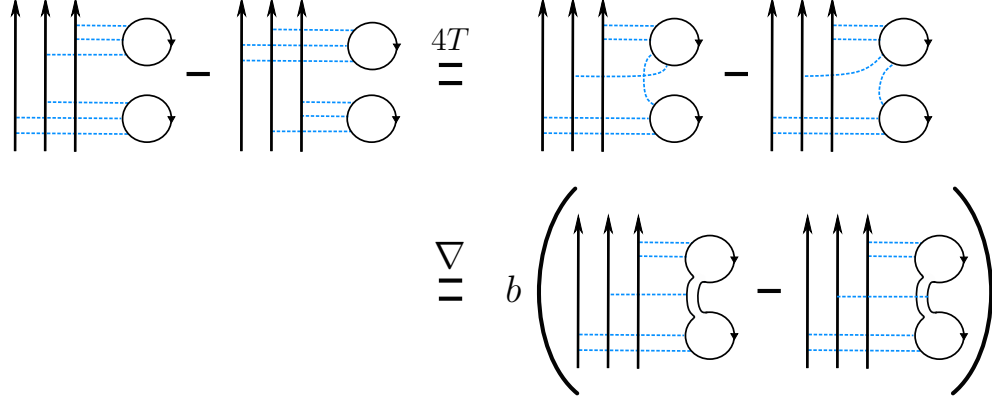


FIGURE 25. Example calculation for the diagrammatic realisation of the graded Goldman bracket.

fig:GradedBracket

hm:Cube\_for\_bracket

**Theorem 5.8.** *The Kontsevich integral descends to a homomorphic expansion for the Goldman bracket, that is, the following diagram commutes:*

$$\begin{array}{ccc}
 |\mathbb{C}\pi| & \xleftarrow{[\cdot, \cdot]_G} & |\mathbb{C}\pi| \otimes |\mathbb{C}\pi| \\
 \downarrow Z/1 & & \downarrow Z/1 \otimes Z/1 \\
 |\widehat{\mathbf{FA}}| & \xleftarrow{\text{gr}[\cdot, \cdot]_G} & |\widehat{\mathbf{FA}}| \otimes |\widehat{\mathbf{FA}}|
 \end{array}$$

*Proof.* The Kontsevich integral is homomorphic with respect to the stacking product (Proposition 4.10). Since  $\lambda$ , the key ingredient in our construction of  $[\cdot, \cdot]_G$ , is the difference between the stacking product and its opposite product,  $Z$  is homomorphic with respect to  $\lambda$ , thus the following square commutes:

$$\begin{array}{ccc}
 & \tilde{\mathcal{T}}_{\nabla}^{/2}(\circ) \otimes \tilde{\mathcal{T}}_{\nabla}^{/2}(\circ) & \\
 & \swarrow \lambda & \downarrow Z/2 \otimes Z/2 \\
 \tilde{\mathcal{T}}_{\nabla}^{/2}(\circ\circ) & & \tilde{\mathcal{A}}_{\nabla}^{/2}(\circ) \otimes \tilde{\mathcal{A}}_{\nabla}^{/2}(\circ) \\
 \downarrow Z/2 & & \swarrow \text{gr } \lambda \\
 \tilde{\mathcal{A}}_{\nabla}^{/2}(\circ\circ) & & 
 \end{array}$$

Hence, we know that that the entire multi-cube (5.3) is commutative: all other faces follow from Theorem 5.5, Corollary 5.6, the fact that  $Z$  is a filtered map with respect to the  $s$ -filtration (Proposition 4.13):

eq:BracketMultiCube

(5.3)

$$\begin{array}{ccccccc}
& \text{Ker} & \longrightarrow & \tilde{\mathcal{T}}_{\nabla}^{1/2}(\mathcal{O}) \otimes \tilde{\mathcal{T}}_{\nabla}^{1/2}(\mathcal{O}) & \longrightarrow & \tilde{\mathcal{T}}^{1/1}(\mathcal{O}) \otimes \tilde{\mathcal{T}}^{1/1}(\mathcal{O}) \\
& \swarrow 0 & \downarrow Z^{1/2} \otimes Z^{1/2} & \swarrow \lambda & \downarrow Z^{1/2} \otimes Z^{1/2} & \swarrow 0 & \downarrow Z^{1/1} \otimes Z^{1/1} \\
\tilde{\mathcal{T}}_{\nabla}^{1/2}(\mathcal{O}\mathcal{O}) & \longrightarrow & \tilde{\mathcal{T}}_{\nabla}^{1/2}(\mathcal{O}\mathcal{O}) & \longrightarrow & \tilde{\mathcal{T}}^{1/1}(\mathcal{O}\mathcal{O}) & \longrightarrow & \tilde{\mathcal{T}}^{1/1}(\mathcal{O}\mathcal{O}) \\
& \downarrow Z^{1/2} & \downarrow \text{Ker} & \downarrow Z^{1/2} & \downarrow Z^{1/1} & \downarrow Z^{1/1} & \downarrow 0 \\
& \swarrow 0 & \longrightarrow & \tilde{\mathcal{A}}_{\nabla}^{1/2}(\mathcal{O}) \otimes \tilde{\mathcal{A}}_{\nabla}^{1/2}(\mathcal{O}) & \longrightarrow & \tilde{\mathcal{A}}^{1/1}(\mathcal{O}) \otimes \tilde{\mathcal{A}}^{1/1}(\mathcal{O}) \\
& \downarrow Z^{1/2} & \downarrow \text{Ker} & \downarrow Z^{1/2} & \downarrow Z^{1/1} & \downarrow Z^{1/1} & \downarrow 0 \\
& \swarrow 0 & \longrightarrow & \tilde{\mathcal{A}}_{\nabla}^{1/2}(\mathcal{O}\mathcal{O}) & \longrightarrow & \tilde{\mathcal{A}}^{1/1}(\mathcal{O}\mathcal{O}) & \longrightarrow & \tilde{\mathcal{A}}^{1/1}(\mathcal{O}\mathcal{O})
\end{array}$$

Hence, using the naturality of the induced map construction (Lemma 2.5 and the diagram (2.4)), we then know that the middle square of (5.4) commutes:

eq:EtaSquare

(5.4)

$$\begin{array}{ccc}
& \tilde{\mathcal{T}}^{1/1}(\mathcal{O}) & \xleftarrow{\hat{\eta}} \tilde{\mathcal{T}}^{1/1}(\mathcal{O}) \otimes \tilde{\mathcal{T}}^{1/1}(\mathcal{O}) \\
& \downarrow Z^{1/1} & \downarrow Z^{1/1} \otimes Z^{1/1} \\
& \tilde{\mathcal{T}}_{\nabla}^{1/2}(\mathcal{O}\mathcal{O}) & \xleftarrow{\eta} \tilde{\mathcal{T}}_{\nabla}^{1/2}(\mathcal{O}\mathcal{O}) \\
& \downarrow Z^{1/2} & \downarrow Z^{1/2} \\
& \tilde{\mathcal{A}}_{\nabla}^{1/2}(\mathcal{O}\mathcal{O}) & \xleftarrow{\text{gr } \eta} \tilde{\mathcal{A}}^{1/1}(\mathcal{O}) \otimes \tilde{\mathcal{A}}^{1/1}(\mathcal{O}) \\
& \uparrow Z^{1/1} & \uparrow Z^{1/1} \\
& \tilde{\mathcal{A}}^{1/1}(\mathcal{O}) & \xleftarrow{\text{gr } \hat{\eta}} \tilde{\mathcal{A}}^{1/1}(\mathcal{O})
\end{array}$$

Since all other faces of the diagram (5.4) are commutative by definition, the outside square also commutes. In turn, this is the middle square of the diagram (5.5):

eq:KIntBracket

(5.5)

$$\begin{array}{ccccccc}
& & & [\cdot, \cdot]_G & & & \\
& \swarrow & & \searrow & & \swarrow & \\
|\mathbb{C}\pi| & \xleftarrow[\beta]{\cong} \tilde{\mathcal{T}}^{1/1}(\mathcal{O}) & \xleftarrow{\hat{\eta}} \tilde{\mathcal{T}}^{1/1}(\mathcal{O}) \otimes \tilde{\mathcal{T}}^{1/1}(\mathcal{O}) & \xleftarrow[\beta^{-1} \otimes \beta^{-1}]{\cong} |\mathbb{C}\pi| \otimes |\mathbb{C}\pi| \\
\downarrow Z^{1/1} & \downarrow Z^{1/1} & \downarrow Z^{1/1} \otimes Z^{1/1} & \downarrow Z^{1/1} \otimes Z^{1/1} \\
|\widehat{\text{FA}}| & \xleftarrow[\text{gr } \beta]{\cong} \tilde{\mathcal{A}}^{1/1}(\mathcal{O}) & \xleftarrow{\text{gr } \hat{\eta}} \tilde{\mathcal{A}}^{1/1}(\mathcal{O}) \otimes \tilde{\mathcal{A}}^{1/1}(\mathcal{O}) & \xleftarrow[\text{gr } \beta^{-1} \otimes \text{gr } \beta^{-1}]{\cong} |\widehat{\text{FA}}| \otimes |\widehat{\text{FA}}| \\
& \swarrow & & \searrow & & \swarrow & \\
& & & \text{gr}[\cdot, \cdot]_G & & & 
\end{array}$$

Once again, all other faces of (5.5) are commutative: by Theorem 5.5 and Corollary 5.6 at the top and bottom; and otherwise by definition. Hence, the outside square commutes, and this is the statement of the theorem.  $\square$

sec:cobacketinCON

**5.2. The Turaev co-bracket.** In Section 3.2 we reviewed the definition of the Turaev cobracket on  $|\mathbb{C}\pi|$  via the map  $\mu : \mathbb{C}\tilde{\pi} \rightarrow |\mathbb{C}\pi| \otimes \mathbb{C}\pi$ , which required choosing a rotation number  $1/2$  representative for curves in  $\mathbb{C}\tilde{\pi}$ . The knot-theoretic version for the cobracket lifts this construction.

We start by interpreting  $\mathbb{C}\tilde{\pi}$  in the context of tangles. Let  $\cap$  denote an interval skeleton component where both endpoints are on the bottom  $D_p \times \{0\}$ . We call a tangle with skeleton  $\cap$  a *bottom tangle*. We mark the endpoints of the interval by  $\bullet$  and  $*$ , as in Figure 26. Furthermore, we denote by  $\tilde{\mathcal{T}}(\mathcal{O}^k \cap^\ell)$  tangles with  $k$  circle skeleton components, and  $\ell$  bottom intervals.

We extend the projection map  $\beta$  (Proposition 5.1) to such tangles to obtain an isomorphism similar to Corollary 5.1:

prop:ascispi

**Proposition 5.9.** *The natural bottom projection, post-composed with closing up open paths by concatenation with paths  $\nu$  from the endpoint to the starting point along the boundary (as in Section 3.2) gives a filtered linear map*

$$\beta : \mathbb{C}\tilde{\mathcal{T}}_{\nabla}(\mathcal{O}^k \cap^\ell) \rightarrow |\mathbb{C}\pi|^{\otimes k} \otimes \mathbb{C}\pi^{\otimes \ell}$$

has kernel  $\tilde{\mathcal{T}}_{\nabla}^{\geq 1}(\mathcal{O}^k \cap^\ell)$ , hence descends to a filtered isomorphism

$$\beta : \tilde{\mathcal{T}}^{1/1}(\mathcal{O}^k \cap^\ell) \xrightarrow{\cong} |\mathbb{C}\pi|^{\otimes k} \otimes \mathbb{C}\pi^{\otimes \ell}.$$

*Proof.* The proof is identical to the proof of Proposition 5.1, aside from the minor issue of base points. In the bottom projection, a tangle strand from  $\bullet$  to  $*$  projects to a homotopy class of a path from  $\bullet$  to  $*$  in  $D_p$ . Such paths are in bijection with  $\mathbb{C}\pi$  via composition with a path  $\nu$  along the boundary from  $*$  to  $\bullet$ .  $\square$

By straightforward inspection of the associated graded map, we obtain:

gr\_beta\_bot\_tangle

**Proposition 5.10.** *The associated graded map*

$$\text{gr } \beta : \tilde{\mathcal{A}}(\mathcal{O}^k \cap^\ell) \rightarrow |\text{FA}|^{\otimes k} \otimes \text{FA}^{\otimes \ell}$$

has kernel  $\tilde{\mathcal{A}}^{\geq 1}(\cap)$ , hence,  $\text{gr } \beta$  descends to a graded isomorphism

$$\text{gr } \beta : \tilde{\mathcal{A}}^{1/1}(\mathcal{O}^k \cap^\ell) \xrightarrow{\cong} |\text{FA}|^{\otimes k} \otimes \text{FA}^{\otimes \ell}.$$

In particular, we have  $\text{gr } \beta : \tilde{\mathcal{A}}^{1/1}(\cap) \xrightarrow{\cong} \text{FA}$ .

We also extend the statements about multiplication and division by  $b$  to the context of mixed skeleta:

op:qbonbottomtangles

**Proposition 5.11.** *The map  $m_b$  descends to  $\mathbb{C}$ -linear isomorphism*

$$m_b : \tilde{\mathcal{T}}_{\nabla}^{1/1}(\cap \cap) \xrightarrow{\cong} \tilde{\mathcal{T}}_{\nabla}^{1/2}(\cap),$$

with inverse map given by  $q_b$ , division by  $b$ .

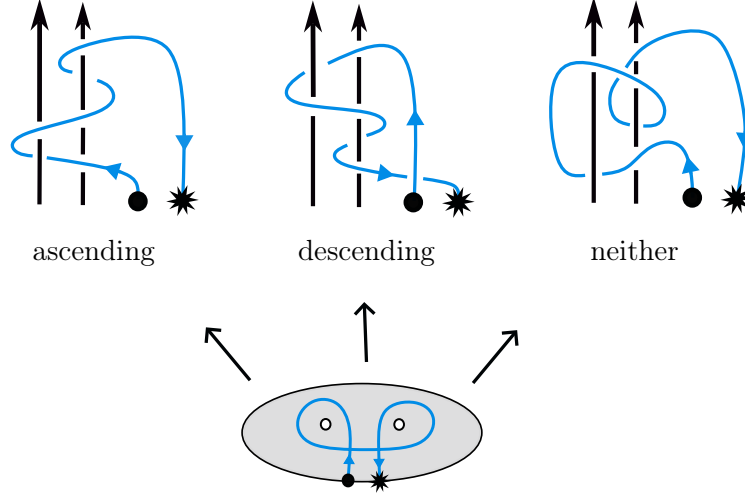


FIGURE 26. A curve in  $\mathbb{C}\pi$  lifted to ascending, descending, and neither ascending nor descending bottom tangles. The three tangles are equivalent in  $\tilde{\mathcal{T}}^{1/1}$ , but distinct in  $\tilde{\mathcal{T}}$ .

fig:ascending

*Proof.* From Corollary 4.20, we know  $m_b$  is a  $\mathbb{C}$ -linear isomorphism  $\tilde{\mathcal{T}}_{\nabla}^{1/1} \xrightarrow{\cong} \tilde{\mathcal{T}}_{\nabla}^{1/2}$ , so we only need to address the change in skeleton. The quotient  $\tilde{\mathcal{T}}_{\nabla}^{1/1}(\bigcirc \cap)$  is generated by classes of tangle diagrams  $D$  with skeleton consisting of one circle and one bottom-to-bottom interval component. After multiplication by  $b$ ,  $b \cdot D$  is equivalent via the Conway relation to a tangle with one double point in  $\tilde{\mathcal{T}}(\cap)$ , as the un-smoothing combines the two skeleton components.  $\square$

Next, we recover the self intersection map  $\mu$ , in the context of tangles, as the connecting homomorphism induced from the difference between two ways to lift a bottom tangle.

Let  $\bullet$  and  $*$  be two “nearby” points on the boundary of  $D_p$ , that is,  $*$  is obtained by shifting  $\bullet$  forwards along the boundary orientation, as shown in Figure 26.

def:asc+desc

**Definition 5.12.** An embedding

$$T : (I, \{0, 1\}) \hookrightarrow (M_p, \{\bullet, *\})$$

(representing a bottom tangle) is called *ascending* if it first ascends monotonically from  $\bullet$ , and then goes *straight* down to  $*$ . More precisely, if  $(z, s)$  is a global coordinate system for  $M_p = D_p \times I$ , then  $T$  is an ascending tangle if there exists  $c \in (0, 1)$  such that when  $t \in (0, c)$ , the  $\frac{d}{ds}$  component of  $\dot{T}$  is positive; when  $t \in (c + \epsilon, 1)$ ,  $\dot{T}$  is a negative constant multiple of  $\frac{d}{ds}$ ; and when  $t \in (c, c + \epsilon)$ ,  $T$  smoothly transitions through a maximum.

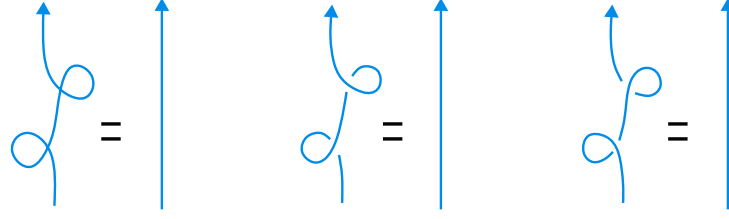


FIGURE 27. Weak R1 moves for regular homotopy curves, framed ascending and framed descending tangles.

raming\_from\_sailing

Likewise, an embedding  $T$  is *descending* if it first goes straight up from  $\bullet$ , then monotonically descends to  $*$ . This can also be made precise as above. See Figure 26 for examples.

**Definition 5.13.** An *ascending tangle* is a bottom tangle in  $M_p$  whose ambient isotopy class has an ascending embedding. Similarly, a *descending tangle* is a bottom tangle in  $M_p$  whose ambient isotopy class has a descending embedding.

In the bottom projection, an ascending embedding will traverse each of its crossings on the under strand first, and on the over strand later. A descending embedding will traverse each crossing on the over strand first.

Given a curve  $\gamma$  in the fundamental group  $\pi = \pi_1(D_p, *)$ ,  $\gamma$  has a unique lift  $\tilde{\gamma}$  in  $\tilde{\pi} = \tilde{\pi}_{\bullet,*}$  with the property that  $\tilde{\gamma} \cdot \nu$  has rotation number zero, where  $\nu$  is a path along the boundary from  $*$  to  $\bullet$ , as in Figure 3. In turn, a rotation number zero curve  $\tilde{\gamma}$  lifts to a well-defined (up to isotopy) framed ascending tangle, where the framing is set to the blackboard framing. Indeed, the weak R1 move for regular isotopy of curves lifts via the ascending lift to the framed R1 move of tangles, as shown in Figure 27. We denote this lift as  $\lambda_a(\gamma)$ . Similarly, there is a well-defined lift  $\lambda_d(\gamma)$  of  $\tilde{\gamma}$  to a framed descending bottom tangle. Via the isomorphism  $\beta$ ,  $\lambda_a$  and  $\lambda_d$  can be seen as maps  $\tilde{\mathcal{T}}^{/1}(\cap) \rightarrow \tilde{\mathcal{T}}^{/2}(\cap)$ . Let  $\bar{\lambda} : \tilde{\mathcal{T}}^{/1}(\cap) \rightarrow \tilde{\mathcal{T}}^{/2}(\cap)$  denote the difference

$$\bar{\lambda}(\gamma) = \lambda_a(\gamma) - \lambda_d(\gamma).$$

Diagrammatically, in the bottom projection one obtains the descending lift from the ascending lift by changing all (strand-strand) crossings.

We are now ready to recover the self-intersection map  $\mu : \mathbb{C}\pi \rightarrow |\mathbb{C}\pi| \otimes \mathbb{C}\pi$  (Definition 3.3).

thm:snake\_for\_mu

**Theorem 5.14.** The map  $\lambda = \bar{\lambda} \circ q$  induces a unique map

$$\hat{\eta} : \tilde{\mathcal{T}}^{/1}(\cap) \rightarrow \tilde{\mathcal{T}}^{/1}(\cap \cap)$$

in the sense of the commutative diagram of Figure 28. The map  $\hat{\eta}$  agrees with the self-intersection map

$$\mu : \mathbb{C}\pi \rightarrow |\mathbb{C}\pi| \otimes \mathbb{C}\pi$$

under the identification  $\beta : \tilde{\mathcal{T}}^{/1}(\cap^k \cap^\ell) \xrightarrow{\cong} |\mathbb{C}\pi|^{\otimes k} \otimes \mathbb{C}\pi^{\otimes \ell}$ , that is,  $\mu = \beta \circ \hat{\eta} \circ \beta^{-1}$ .



$$\begin{array}{ccccccc}
& & \tilde{\mathcal{T}}_{\nabla}^{1/2}(\cap) & \xrightarrow{\quad} & \tilde{\mathcal{T}}_{\nabla}^{1/2}(\cap) & \xrightarrow{q} & \tilde{\mathcal{T}}^{1/1}(\cap) \longrightarrow 0 \\
& & \downarrow 0 & & \downarrow \lambda = \bar{\lambda} \circ q & \swarrow \bar{\lambda} & \downarrow 0 \\
0 \longrightarrow & \tilde{\mathcal{T}}_{\nabla}^{1/2}(\cap) & \longrightarrow & \tilde{\mathcal{T}}_{\nabla}^{1/2}(\cap) & \longrightarrow & \tilde{\mathcal{T}}^{1/1}(\cap) \\
& \downarrow q_b & & & & & \\
& \tilde{\mathcal{T}}^{1/1}(\bigcirc \cap) & \xleftarrow{\quad} & & & & 
\end{array}$$

$\eta$  (dashed arrow from  $\tilde{\mathcal{T}}_{\nabla}^{1/2}(\cap)$  to  $\tilde{\mathcal{T}}^{1/1}(\bigcirc \cap)$ )  
 $\hat{\eta}$  (dashed arrow from  $\tilde{\mathcal{T}}^{1/1}(\cap)$  to  $\tilde{\mathcal{T}}^{1/1}(\bigcirc \cap)$ )

FIGURE 28. The nontrivial horizontal maps are the respective quotient maps, and  $q$  is one such quotient map.

fig:Snakeformu

*Proof.* We first show that the diagram of Figure 28 commutes. The commutativity of the left square is immediate from the exactness of the top row. The right side square is split into two triangles: of these the top one commutes by definition. The commutativity of the bottom triangle, that is, the fact that the post-composition of  $\bar{\lambda}$  with the projection to  $\tilde{\mathcal{T}}^{1/1}(\cap)$  is the zero map, is also straightforward, as follows. For a curve  $\gamma$  in  $\tilde{\mathcal{T}}^{1/1}(\cap) \cong \mathbb{C}\pi$ , the map  $\bar{\lambda}$  is the difference of two lifts of  $\gamma$  to bottom tangles. When these lifts are subsequently projected back to  $\tilde{\mathcal{T}}^{1/1}(\cap)$ , they both project to  $\gamma$ , hence, their difference is 0.

Thus, as in Section 2, diagram (2.1),  $\lambda$  induces a unique well defined homomorphism  $\eta : \tilde{\mathcal{T}}^{1/1}(\cap) \rightarrow \tilde{\mathcal{T}}_{\nabla}^{1/2}(\cap)$ . By Proposition 5.11, the division by  $b$  map  $q_b$  restricts to an isomorphism  $q_b : \tilde{\mathcal{T}}_{\nabla}^{1/2}(\cap) \rightarrow \tilde{\mathcal{T}}^{1/1}(\bigcirc \cap)$ . The map  $\hat{\eta} : \tilde{\mathcal{T}}^{1/1}(\cap) \rightarrow \tilde{\mathcal{T}}^{1/1}(\bigcirc \cap)$  is the composition  $\hat{\eta} = q_b \circ \eta$ .

It remains to show that  $\mu = \beta \circ \hat{\eta} \circ \beta^{-1}$ . Given a curve  $\gamma \in |\mathbb{C}\pi|$ , the value of  $\beta \circ \hat{\eta} \circ \beta^{-1}$  is calculated as follows:  $\gamma$  is lifted to a curve of rotation number zero in  $\tilde{\pi} = \tilde{\pi}_{\bullet*}$ , and, in turn, interpreted as an element in  $\tilde{\mathcal{T}}^{1/1}(\cap)$ . The map  $\bar{\lambda}$  is applied to this framed curve, to obtain a difference of tangles in  $\tilde{\mathcal{T}}_{\nabla}^{1/2}(\cap)$ . This value is divided by  $b$ , and interpreted as a loop and a curve in  $|\mathbb{C}\pi| \otimes \mathbb{C}\pi$ .

Let  $\gamma$  be a curve in  $\tilde{\mathcal{T}}^{1/1}(\cap) \cong \mathbb{C}\pi$ , and let  $\lambda_a(\gamma) = T_a$  be the framed ascending lift of  $\gamma$  and  $\lambda_d(\gamma) = T_d$  the framed descending lift. Then  $\bar{\lambda}(\gamma) = T_a - T_d$ . Denote the bottom projection of  $T_a$  by  $D_a$ , and the bottom projection of  $T_d$  by  $D_d$ . In particular,  $D_d$  coincides with  $D_a$ , but with all crossings flipped.

As in the proof of Theorem 5.5, number the mixed crossings of  $D_a$  from 1 to  $r$ , and let  $D_i$  denote the link diagram where the first  $i$  mixed crossings have been flipped. Specifically,  $D_0 = D_a$  and  $D_r = D_d$ . Then  $D_0 - D_r$  can be written as a telescopic sum:

eq:Telescope2

$$(5.6) \quad D_0 - D_r = (D_0 - D_1) + (D_1 - D_2) + \dots + (D_{r-1} - D_r).$$

$$= b \left( \text{Diagram 1} - \text{Diagram 2} \right)$$

```
fig:CobrocketCalc
```

In the sum (5.6) each term  $(D_i - D_{i+1})$  contains one (signed) double point corresponding to a self-intersection of  $\gamma$ . We apply the Conway relation  $(\bowtie = b \cdot \smile)$  at these double points. A straightforward check shows that the sign arising from the crossing signs matches the sign  $-\varepsilon_p$  in the definition of  $\mu$  (Definition 3.3). Thus, dividing by  $b$  and reinterpreting via  $\beta$  coincides with the value of  $\mu(\gamma)$ , as required: see Figure 29 for an illustration.

It will be necessary for proving the formality statement – that is, the compatibility with the Kontsevich integral – to also have a concrete understanding of the associated graded map of  $\lambda$ . Recall from 5.4 and Proposition 5.10 that in  $\tilde{\mathcal{A}}^1$  chord endings commute on the poles: this gives the isomorphism  $\mathrm{gr} \beta : \tilde{\mathcal{A}}^1(\bigcirc) \rightarrow \mathrm{FA}$ .

**Lemma 5.15.** *Given a chord diagram  $D \in \tilde{\mathcal{A}}^1(\cap)$ , the map  $\text{gr } \lambda_a : \tilde{\mathcal{A}}^1 \rightarrow \tilde{\mathcal{A}}_{\nabla}^{1/2}$  orders the chord endings of  $D$  in an ascending order along the poles, that is, the ordering along the poles match the ordering along the strand. Similarly,  $\text{gr } \lambda_a : \tilde{\mathcal{A}}^1 \rightarrow \tilde{\mathcal{A}}_{\nabla}^{1/2}$  orders the chord endings of  $D$  along the poles in a descending order, that is, opposite to the ordering along the strand.*

*Proof.* This is immediate from the definition of the associated graded map: choose a singular tangle  $T_D$  representing  $D$ , and inspect the chord diagram representing  $\lambda_a(T_D)$  (respectively,  $\lambda_d(T_D)$ ).  $\square$

As with the Goldman bracket, the associated graded version of the same statement follows immediately:

**Corollary 5.16.** *The diagram in Figure 30 commutes, the rows are exact,  $\text{gr } \eta$  is the induced homomorphism, and  $\text{gr } \mu = \text{gr } \beta \circ \text{gr } \hat{\eta} \circ (\text{gr } \beta)^{-1}$ .*

$$\begin{array}{ccccccc}
\tilde{\mathcal{A}}_{\nabla}^{1/2}(\cap) & \longrightarrow & \tilde{\mathcal{A}}_{\nabla}^{1/2}(\cap) & \longrightarrow & \tilde{\mathcal{A}}^1(\cap) & \longrightarrow & 0 \\
\downarrow 0 & & \downarrow \text{gr } \lambda & & \downarrow 0 & & \\
0 & \longrightarrow & \tilde{\mathcal{A}}_{\nabla}^{1/2}(\cap) & \longrightarrow & \tilde{\mathcal{A}}_{\nabla}^{1/2}(\cap) & \longrightarrow & \tilde{\mathcal{A}}^1(\cap) \\
& & \downarrow \text{gr } q_b & & & & \\
& & \tilde{\mathcal{A}}^1(\cap) & \xleftarrow{\text{gr } \hat{\eta}} & & & 
\end{array}$$

FIGURE 30. Associated graded diagram constructing the graded self-intersection map.

akefor\_gr\_cobacket

$$\begin{array}{ccc}
\tilde{\mathcal{T}}^{1/1}(\cap) & \xrightarrow{\hat{\eta}} & \tilde{\mathcal{T}}^{1/1}(\cap) \\
\downarrow cl & \searrow \hat{\zeta} & \downarrow cl \\
& & \tilde{\mathcal{T}}^{1/1}(\cap) \otimes \tilde{\mathcal{T}}^{1/1}(\cap) \\
& \searrow \tilde{\zeta} & \downarrow Alt \\
\tilde{\mathcal{T}}^{1/1}(\cap) & \xrightarrow{\zeta} & \tilde{\mathcal{T}}^{1/1}(\cap) \otimes \tilde{\mathcal{T}}^{1/1}(\cap)
\end{array}$$

This can be in the text.

fig:CobacketSteps

FIGURE 31. Constructing  $\zeta$  from  $\hat{\eta}$ .

*Proof.* This follows from general principles in exactly the same way as Corollary 5.6.  $\square$

Recall from Section 3.2 that the Turaev cobracket  $\delta : |\mathbb{C}\pi| \rightarrow |\mathbb{C}\pi| \otimes |\mathbb{C}\pi|$  is constructed from  $\mu : \mathbb{C}\pi \rightarrow |\mathbb{C}\pi| \otimes \mathbb{C}\pi$ . One post-composes  $\mu$  with the trace map  $\mathbb{C}\pi \rightarrow |\mathbb{C}\pi|$  in the second component, then antisymmetrises using the map  $Alt(x \otimes y) = x \otimes y - y \otimes x$ . The composition  $\hat{\delta} = Alt \circ |\cdot| \circ \mu : \mathbb{C}\pi \rightarrow |\mathbb{C}\pi| \otimes |\mathbb{C}\pi|$  descends to the Turaev cobracket  $\delta$ .

We mimic this construction in the context of tangle diagrams by post-composing  $\hat{\eta}$  with the closure map  $cl : \tilde{\mathcal{T}}(\cap) \rightarrow \tilde{\mathcal{T}}(\cap)$  on the open component, followed by anti-symmetrising, as shown in the diagram in Figure 31. The closure map connects the endpoints of the bottom tangle,  $\bullet$  and  $*$ , by the path  $\nu$  connecting  $*$  to  $\bullet$  along the bottom boundary  $\partial D_p$ , following the orientation (as in Figure 3). We denote the map  $cl \circ \hat{\eta} =: \hat{\zeta}$ , and after antisymmetrisation  $Alt \circ \hat{\zeta} =: \tilde{\zeta}$ . We will show that  $\tilde{\zeta}$  descends to a map  $\zeta : \tilde{\mathcal{T}}^{1/1}(\cap) \rightarrow \tilde{\mathcal{T}}^{1/1}(\cap) \otimes \tilde{\mathcal{T}}^{1/1}(\cap)$ , which realises the Turaev cobracket via the identification  $\beta$ .

DROR SIGNED OFF  
HERE

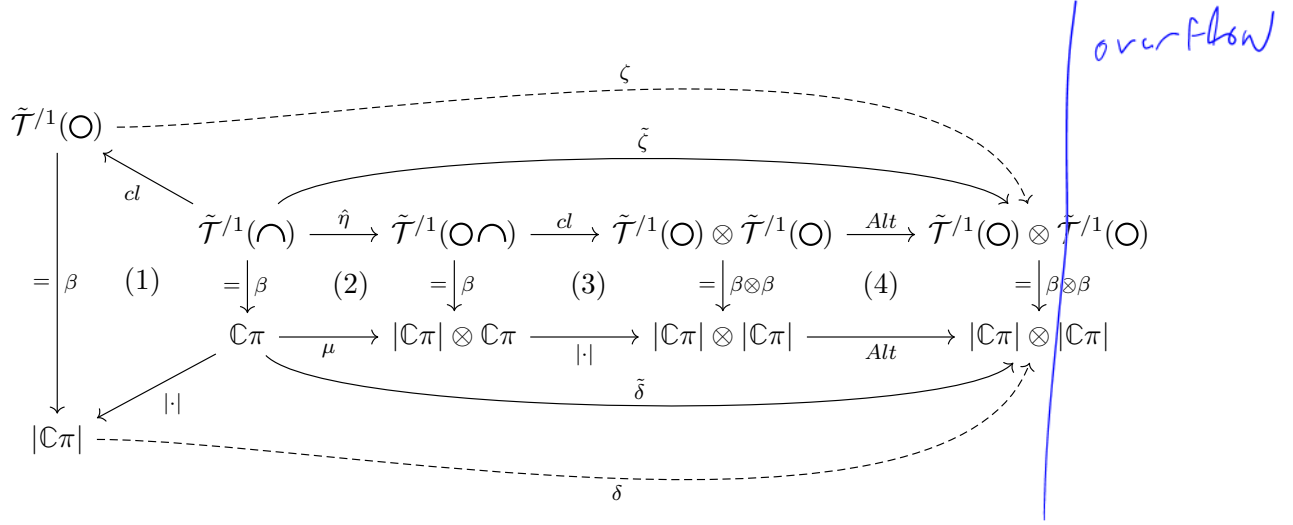
FIGURE 32. The map  $\zeta$  realises the Turaev cobracket  $\delta$ .

fig:Identifications

**Proposition 5.17.** *The map  $\zeta$  realises the Turaev cobracket  $\delta$  via the identifications  $\beta$ , in the sense that the diagram in Figure 32 commutes.*

*Proof.* The only substantial statement is the commutativity of the square (2): this is Theorem 5.14. Squares (1) and (3) are the same: the closure map corresponds to the trace  $\mathbb{C}\pi \rightarrow |\mathbb{C}\pi|$ , which is a basic homotopy fact. Square (4) is tautological. The maps  $\tilde{\zeta}$  and  $\tilde{\delta}$  are defined as the compositions shown, in particular, we have  $\tilde{\delta} = (\beta \otimes \beta) \circ \tilde{\zeta} \circ \beta^{-1}$ . The fact that  $\tilde{\delta}$  descends to  $\delta$  is Proposition 5.10 of [AKKN18b]. The fact that  $\tilde{\zeta}$  descends to  $\zeta$  is immediate from the canonical identifications.  $\square$

**Corollary 5.18.** *The corresponding statement is true for the associated graded cobracket:*

$$\text{gr } \delta = (\text{gr } \beta \otimes \text{gr } \beta) \circ \text{gr } \zeta \circ \text{gr } \beta^{-1}.$$

 $\square$ 

The key result left to prove is that  $\zeta$  is homomorphic with respect to the Kontsevich integral  $Z$ :  $\text{gr } \zeta \circ Z = Z \circ \zeta$ , and hence the Kontsevich integral descends to a homomorphic expansion for  $\delta$ . The subtlety involved is that  $Z$  does *not* respect the map  $\hat{\eta}$  – there is an error term –, but this error term cancels after applying the closure to obtain  $\hat{\zeta}$ , and hence true for the corresponding *ordered* version of the Turaev cobracket. Hence, we will prove the homomorphicity of  $Z$  with respect to  $\hat{\zeta}$ , and the rest follows from this for free.

To prove that  $Z$  is homomorphic with respect to  $\hat{\zeta}$ , we want to use the naturality of the induced homomorphism, as outlined in Section 2 and demonstrated in

Section 5.1 for the Goldman bracket. The idea would be to prove that all faces of a multi-cube similar to (5.3) commute. As before, the only non-trivial part of this statement is the commutativity of the middle square involving the map  $\lambda$ ; unfortunately, in the case of the self-intersection map, this square fails to commute:

eq:FailToCommute

(5.7)

$$\begin{array}{ccc}
 & \tilde{\mathcal{T}}_{\nabla}^{/2}(\cap) & \\
 & \swarrow \lambda & \downarrow Z^{/2} \\
 \tilde{\mathcal{T}}_{\nabla}^{/2}(\cap) & & \tilde{\mathcal{A}}_{\nabla}^{/2}(\cap) \\
 \downarrow Z^{/2} & \searrow \text{gr } \lambda & \\
 \tilde{\mathcal{A}}_{\nabla}^{/2}(\cap) & & 
 \end{array}$$

add some notation for "does not commute".

This failure is mirrored in the setting of the Goldman–Turaev Lie bialgebra by the fact the the self-intersection map  $\mu$  is *not formal*, only the Turaev cobracket obtained from it is [AKKN18b].

The resolution of this issue comes down to two observations:

- (1) The square (5.7) fails to commute by a controlled error; and
- (2) after applying the closure map, this error vanishes.

The next lemma addresses the first of these steps by modifying the bottom arrow of (5.7) to correct the error:

**Lemma 5.19.** *There exists a map  $\lambda^{alg} : \tilde{\mathcal{A}}_{\nabla}^{/2}(\cap) \rightarrow \tilde{\mathcal{A}}_{\nabla}^{/2}(\cap)$  so that the diagram (5.9) commutes. (or course,  $\lambda^{alg} \neq \text{gr } \lambda$ ).*

eq:FixedSquare

(5.8)

$$\begin{array}{ccc}
 \tilde{\mathcal{T}}_{\nabla}^{/2}(\cap) & \xleftarrow{\lambda} & \tilde{\mathcal{T}}_{\nabla}^{/2}(\cap) \\
 \downarrow Z^{/2} & & \downarrow Z^{/2} \\
 \tilde{\mathcal{A}}_{\nabla}^{/2}(\cap) & \xleftarrow{\lambda^{alg}} & \tilde{\mathcal{A}}_{\nabla}^{/2}(\cap)
 \end{array}$$

opposite composition!

*Proof.* Recall that by definition,  $\lambda = (\lambda_a - \lambda_d) \circ q$ , where  $q$  is the projection to  $\tilde{\mathcal{T}}^{/1}(\cap)$ , and  $\lambda_a$  and  $\lambda_d$  are the ascending and descending lifts. Since the Kontsevich integral is compatible with the  $s$ -filtration and hence  $q$ , it is enough to show the analogous statements for  $\lambda_a$  and  $\lambda_d$ , namely, that there exist maps  $\lambda_a^{alg}$  and  $\lambda_d^{alg}$  making the following squares commute:

eq:FixedSquare

(5.9)

$$\begin{array}{ccc}
 \tilde{\mathcal{T}}_{\nabla}^{/2}(\cap) & \xleftarrow{\lambda_a} & \tilde{\mathcal{T}}_{\nabla}^{/1}(\cap) \\
 \downarrow Z^{/2} & & \downarrow Z^{/1} \\
 \tilde{\mathcal{A}}_{\nabla}^{/2}(\cap) & \xleftarrow{\lambda_a^{alg}} & \tilde{\mathcal{A}}_{\nabla}^{/1}(\cap)
 \end{array}
 \qquad
 \begin{array}{ccc}
 \tilde{\mathcal{T}}_{\nabla}^{/2}(\cap) & \xleftarrow{\lambda_d} & \tilde{\mathcal{T}}_{\nabla}^{/1}(\cap) \\
 \downarrow Z^{/2} & & \downarrow Z^{/1} \\
 \tilde{\mathcal{A}}_{\nabla}^{/2}(\cap) & \xleftarrow{\lambda_d^{alg}} & \tilde{\mathcal{A}}_{\nabla}^{/1}(\cap)
 \end{array}$$

fig:AscDecomp

FIGURE 33. Tangle decomposition of the ascending lift  $\lambda_a(\gamma)$ .

FIGURE 34. Tangle decomposition of the descending lift.

} missing!

Let  $\gamma$  be a curve in  $\tilde{\mathcal{T}}^{/1}(\cap)$ . To find  $\lambda_a^{alg}$ , we need to express  $Z^{/2}(\lambda_a(\gamma))$  in terms of  $Z^{/1}(\gamma)$ . Since the Kontsevich integral is compatible with the  $s$ -filtration,  $Z^{/1}(\gamma) = Z^{/1}(\lambda_a(\gamma))$ .

The proof thus depends on understanding the Kontsevich integral of  $\lambda_a(\gamma)$ : see Figure 33 for an expression as the tangle composition

$$\text{eq:Asc} \quad (5.10) \quad \lambda_a(\gamma) = \Phi_1 \beta \Phi_2 C.$$

Since the Kontsevich integral is multiplicative with respect to tangle composition,

$$\text{eq:ZAsc} \quad (5.11) \quad Z^{/2}(\lambda_a(\gamma)) = Z^{/2}(\Phi_1) Z^{/2}(\beta) Z^{/2}(\Phi_2) Z^{/2}(C).$$

Since the Kontsevich integral asymptotically commutes with “distant disjoint unions” [CDM12, Chapter 8], the values of  $C$  and  $\beta$  include only chords in the highlighted areas of Figure 33. In particular, the value of the cap in  $C$  includes strand-strand chords only, and has no degree one term [BNGRT00], thus,  $Z^{/2}(C) = 1$ . As for  $\beta$ ,  $Z^{/2}(\beta)$  has no strand-strand chords, and the strand-pole chords follow the strand in ascending order. Thus, by Lemma 5.15,

$$\text{eq:Zbeta} \quad (5.12) \quad Z^{/2}(\beta) = \text{gr } \lambda_a(Z^{/1}(\gamma)).$$

Combining (5.11) and (5.12), we have

$$(5.13) \quad Z^{/2}(\lambda_a(\gamma)) = Z^{/2}(\Phi_1) \text{gr } \lambda_a Z^{/1}(\gamma) Z^{/2}(\Phi_2)$$

Thus,

$$\text{eq:AscAlg} \quad (5.14) \quad \lambda_a^{alg}(D) = Z^{/2}(\Phi_1) \text{gr } \lambda_a(D) Z^{/2}(\Phi_2)$$

completes the commutative diagram (5.9) for  $\lambda_a$ , as required.

Similarly for  $\lambda_d(\gamma)$ , Figure ?? shows that

$$\text{eq:ZDesc} \quad (5.15) \quad Z^{/2}(\lambda_d(\gamma)) = Z^{/2}(\Phi_1) Z^{/2}(\Phi_2) Z^{/2}(R) Z^{/2}(\Phi_2)^{-1} Z^{/2}(\beta) Z^{/2}(\Phi_2)$$

By the same reasoning as before,  $Z(R)$  consists only of strand-strand chords. The Kontsevich integral of a negative crossing is easy to compute explicitly, and, up to  $s$ -degree two,  $Z^{/2}(R) = 1 - c/2$ , where  $c$  denotes a single chord between the two crossing strands. Substituting this in, we obtain:

$$Z^{/2}(\lambda_d(\gamma)) = Z^{/2}(\Phi_1) Z^{/2}(\beta) Z^{/2}(\Phi_2) - Z^{/2}(\Phi_1) Z^{/2}(\Phi_2) \frac{c}{2} Z^{/2}(\Phi_2)^{-1} Z^{/2}(\beta) Z^{/2}(\Phi_2)$$

To simplify the second term, keep in mind that the product is valued in  $\tilde{\mathcal{A}}^{/2}(\cap)$ , and the chord  $c$  is in  $s$ -degree 1. Therefore, we only need to consider the  $s$ -degree

zero parts of the other terms. It is a property of the Kontsevich integral that deleting either of the (non-pole) strands of either  $Z(\Phi_1)$  or  $Z(\Phi_2)$  simplifies to 1; therefore, the  $s$ -degree zero components of these values is 1. Thus, we have

$$\boxed{\text{eq:ZDescSimp}} \quad (5.16) \quad Z^{/2}(\lambda_d(\gamma)) = Z^{/2}(\Phi_1)Z^{/2}(\beta)Z^{/2}(\Phi_2) - \frac{c}{2}Z^{/2}(\beta)$$

In summary,

$$\boxed{\text{eq:DescAlg}} \quad (5.17) \quad \lambda_d^{alg}(D) = Z^{/2}(\Phi_1) \text{gr } \lambda_d(D) Z^{/2}(\Phi_2) - \frac{c}{2} \text{gr } \lambda_d(D),$$

as required.  $\square$

Zsuzsi edited to here

obackethomomorphic

**Theorem 5.20.** *The Kontsevich integral descends to a homomorphic expansion for the ordered Turaev cobracket. That is, the outside square of following diagram commutes:*

$$\begin{array}{ccccccc}
 & & & \hat{\delta} & & & \\
 & \swarrow & & \searrow & & \swarrow & \\
 \mathbb{C}\pi \otimes \mathbb{C}\pi & \xleftarrow[\beta \otimes \beta]{\cong} & \tilde{\mathcal{T}}^{/1}(\bigcirc) \otimes \tilde{\mathcal{T}}^{/1}(\bigcirc) & \xleftarrow[\hat{\zeta}]{} & \tilde{\mathcal{T}}^{/1}(\frown) & \xleftarrow[\beta^{-1}]{\cong} & \mathbb{C}\pi \\
 \downarrow Z^{/1} \otimes Z^{/1} & & \downarrow Z^{/1} \otimes Z^{/1} & & \downarrow Z^{/1} & & \downarrow Z^{/1} \\
 \widehat{\text{FA}} \otimes \widehat{\text{FA}} & \xleftarrow[\text{gr } \beta \otimes \text{gr } \beta]{\cong} & \mathcal{A}^{/1}(\bigcirc) \otimes \mathcal{A}^{/1}(\bigcirc) & \xleftarrow[\text{gr } \hat{\zeta}]{} & \mathcal{A}^{/1}(\frown) & \xleftarrow[\text{gr } \beta^{-1}]{\cong} & \widehat{\text{FA}} \\
 & \nwarrow & & \nearrow & & \nwarrow & \\
 & & & \text{gr } \hat{\delta} & & & 
 \end{array}$$

*Proof.* In the diagram above, the top and bottom squares commute by Theorem 5.14 and Corollary ?? . The right and left square trivially commute because  $\beta$  is a filtered isomorphism. All that remains to be shown is the commutativity of the middle square. This middle square occurs as the diagonal square of the multi-cube in Figure 35.

The diagram in Figure 35 is attained by taking the Kontsevich integral of the commutative diagram in Figure ?? (with the middle layers omitted). We have already established that the top and bottom faces commute by Lemma ?? and Lemma ?? . The left and right vertical sides trivially commute because of the zero maps. The front-left vertical square commutes by Lemma ?? . The front-right and back faces commute because  $Z$  respects the  $s$ -filtration and is homomorphic with respect to the inclusion and quotient maps of the filtered components.

The middle vertical face of Figure 35 is the following square.

Technically we did not show the top square commutes. We showed the top square with  $\mu$  commutes and then show how we build  $\hat{\delta}$  from  $\mu$ . I'm wondering if we should add in a corollary stating exactly that the top square commutes, or just cite to Theorem 5.14 I'm not sure what the correct argument here should be, but it is something somewhat trivial.

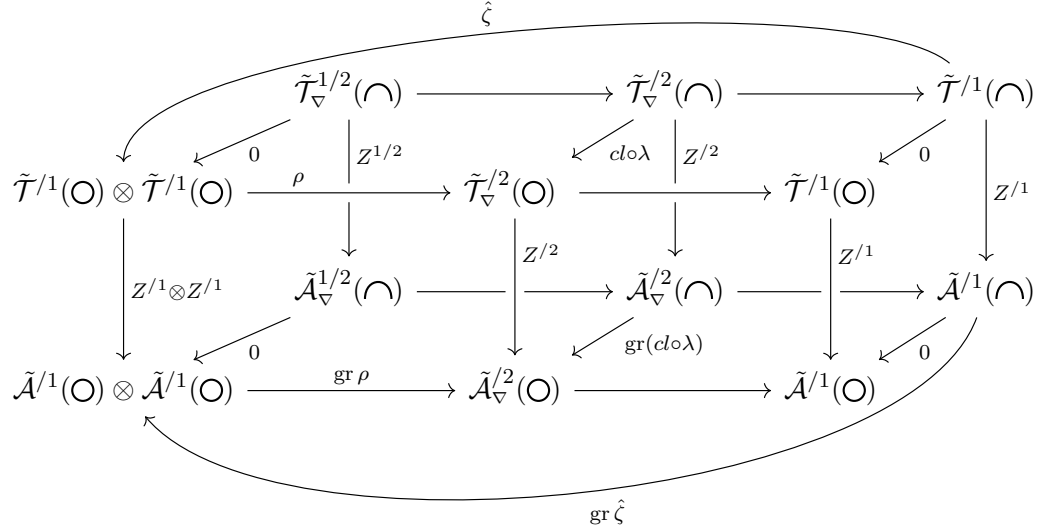


FIGURE 35. Commutative cube showing the formality of the ordered Turaev cobracket from the Kontsevich integral.

:Cube\_for\_cobracket

$$\begin{array}{ccc}
 & & \tilde{\mathcal{T}}_{\nabla}^{2/2}(\cap) \\
 & \swarrow^{cl \circ \lambda} & \downarrow Z^{2/2} \\
 \tilde{\mathcal{T}}_{\nabla}^{2/2}(\circ) & & \mathcal{A}_{\nabla}^{2/2}(\cap) \\
 \downarrow Z^{2/2} & \swarrow_{\text{gr}(cl \circ \lambda)} & \\
 \mathcal{A}_{\nabla}^{2/2}(\circ) & & 
 \end{array}$$

The Kontsevich integral is homomorphic with respect to the flip operation, as shown in Proposition 4.10. The map  $cl \circ \lambda$  applied to a bottom tangle outputs the difference between the closed ascending lift and the closed descending lift. The closed descending lift is the flip of the closed ascending lift. So  $cl \circ \lambda = (id - flip) \circ cl$  acting on ascending representatives.  $Z$  is homomorphic with respect to  $(id - flip) \circ cl$ .

The commutativity of all vertical faces of the cube diagram in Figure 35 implies that the induced diagonal square also commutes, which gives the desired formality of the theorem statement.  $\square$

remark—if we were doing this with  $\mu$  it wouldn't work because flip of a bottom tangle is not a bottom tangle. It is much cleaner to just pass to the closures.

This is not quite right,  
FIX ME!

where does conjugation  
come into play??  
Something about flipping  
first then dragging the  
ends down and then  
closing.



## REFERENCES

- |                                                                                                 |           |                                                                                                                                                                                                                |
|-------------------------------------------------------------------------------------------------|-----------|----------------------------------------------------------------------------------------------------------------------------------------------------------------------------------------------------------------|
| <div style="border: 1px solid black; padding: 2px; display: inline-block;">AKKN_highergen</div> | [AKKN18a] | Anton Alekseev, Nariya Kawazumi, Yusuke Kuno, and Florian Naef. The goldman-turaev lie bialgebra and the kashiwara-vergne problem in higher genera, 2018.                                                      |
| <div style="border: 1px solid black; padding: 2px; display: inline-block;">akkn_g0</div>        | [AKKN18b] | Anton Alekseev, Nariya Kawazumi, Yusuke Kuno, and Florian Naef. The goldman-turaev lie bialgebra in genus zero and the kashiwara-vergne problem. <i>Advances in Mathematics</i> , 326:1–53, 2018.              |
| <div style="border: 1px solid black; padding: 2px; display: inline-block;">AKKN_formality</div> | [AKKN20]  | Anton Alekseev, Nariya Kawazumi, Yusuke Kuno, and Florian Naef. Goldman-turaev formality implies kashiwara-vergne. <i>Quantum Topology</i> , 11(4):657–689, 2020.                                              |
| <div style="border: 1px solid black; padding: 2px; display: inline-block;">BN1</div>            | [BN95]    | D. Bar-Natan. On the vassiliev knot invariants. <i>Topology</i> , 34:423–472, 1995.                                                                                                                            |
| <div style="border: 1px solid black; padding: 2px; display: inline-block;">WK02</div>           | [BND17]   | Dror Bar-Natan and Zsuzsanna Dancso. Finite type invariants of w-knotted objects II: tangles, foams and the Kashiwara-Vergne problem. <i>Math. Ann.</i> , 367(3-4):1517–1586, 2017.                            |
| <div style="border: 1px solid black; padding: 2px; display: inline-block;">BN2</div>            | [BNGRT00] | Dror Bar-Natan, Stavros Garoufalidis, Lev Rozansky, and Dylan P. Thurston. Wheels, wheeling, and the kontsevich integral of the unknot. <i>Israel Journal of Mathematics</i> , 119:217–237, 2000.              |
| <div style="border: 1px solid black; padding: 2px; display: inline-block;">CDM_2012</div>       | [CDM12]   | S. Chmutov, S. Duzhin, and J. Mostovoy. <i>Introduction to Vassiliev Knot Invariants</i> . Cambridge University Press, 2012.                                                                                   |
| <div style="border: 1px solid black; padding: 2px; display: inline-block;">Da</div>             | [Dan10]   | Zsuzsanna Dancso. On the kontsevich integral for knotted trivalent graphs. <i>Alg. Geom. Topol.</i> , 10(3):1317–1365, 2010.                                                                                   |
| <div style="border: 1px solid black; padding: 2px; display: inline-block;">Gol</div>            | [Gol86]   | William Mark Goldman. Invariant functions on lie groups and hamiltonian flows of surface group representations. <i>Invent. Math.</i> , 85:263–302, 1986.                                                       |
| <div style="border: 1px solid black; padding: 2px; display: inline-block;">Gor</div>            | [Gor99]   | Viktor Goryunov. Vassiliev invariants of knots in $\mathbb{R}^3$ and in a solid torus. <i>Differential and symplectic topology of knots and curves</i> , <i>Amer. Math. Soc. Transl.</i> , 190(2):37–59, 1999. |
| <div style="border: 1px solid black; padding: 2px; display: inline-block;">HM</div>             | [HM21]    | Kazuo Habiro and Gwénaél Massuyeau. The Kontsevich integral for bottom tangles in handlebodies. <i>Quantum Topol.</i> , 12(4):593–703, 2021.                                                                   |
| <div style="border: 1px solid black; padding: 2px; display: inline-block;">Kon</div>            | [Kon93]   | Maxim Kontsevich. Vassiliev’s knot invariants. <i>Adv. in Soviet Math.</i> , 16(2):137–150, 1993.                                                                                                              |
| <div style="border: 1px solid black; padding: 2px; display: inline-block;">LM95</div>           | [LM95]    | Tu Quoc Thang Le and Jun Murakami. Kontsevich’s integral for the homfly polynomial and relations between values of multiple zeta functions. <i>Topology and its applications</i> , 62:193–206, 1995.           |
| <div style="border: 1px solid black; padding: 2px; display: inline-block;">LM96</div>           | [LM96]    | Tu Quoc Thang Le and Jun Murakami. The universal Vassiliev-Kontsevich invariant for framed oriented links. <i>Compositio Mathematica</i> , 102(1):41–64, 1996.                                                 |
| <div style="border: 1px solid black; padding: 2px; display: inline-block;">Mag</div>            | [Mag35]   | W Magnus. Beziehungen zwischen gruppen und idealen in einem speziellen ring. <i>Mathematische Annalen</i> , 111:259–280, 1935.                                                                                 |
| <div style="border: 1px solid black; padding: 2px; display: inline-block;">Mas</div>            | [Mas18]   | Géwnael Massuyeau. Formal descriptions of turaev’s loop operations. <i>Quantum Topol.</i> , 9:39–117, 2018.                                                                                                    |
| <div style="border: 1px solid black; padding: 2px; display: inline-block;">Tur</div>            | [Tur91]   | Vladimir Turaev. Skein quantization of poisson algebras of loops on surfaces. <i>Ann. Sci. École Norm. Sup.</i> , 24:635–704, 1991.                                                                            |

DEPARTMENT OF MATHEMATICS, UNIVERSITY OF TORONTO, TORONTO, ONTARIO, CANADA

*Email address:* `drorbn@math.toronto.edu`

*URL:* `http://www.math.toronto.edu/~drorbn`

SCHOOL OF MATHEMATICS AND STATISTICS, THE UNIVERSITY OF SYDNEY, SYDNEY, NSW,  
AUSTRALIA

*Email address:* `zsuzsanna.dancso@sydney.edu.au`

SCHOOL OF MATHEMATICS AND STATISTICS, THE UNIVERSITY OF MELBOURNE, MEL-  
BOURNE, VICTORIA, AUSTRALIA

*Email address:* `hogant@student.unimelb.edu.au`

*URL:* `https://www.tamaramaehogan.com/`

DEPARTMENT OF MATHEMATICS, UNIVERSITY OF TORONTO, TORONTO, ONTARIO, CANADA

*Email address:* `chengjin.liu@mail.utoronto.ca`

DEPARTMENT OF MATHEMATICS AND STATISTICS, ELON UNIVERSITY, ELON, NORTH CAR-  
OLINA

*Email address:* `nscherich@elon.edu`

*URL:* `http://www.nancyscherich.com`